JOURNAL OF THE AMERICAN WATER RESOURCES ASSOCIATION

Vol. 50, No. 3 AMERICAN WATER RESOURCES ASSOCIATION June 2014

LONG-TERM HIGH-RESOLUTION RADAR RAINFALL FIELDS FOR URBAN HYDROLOGY[1]

Daniel B. Wright, James A. Smith, Gabriele Villarini, and Mary Lynn Baeck[2]

ABSTRACT: Accurate records of high-resolution rainfall fields are essential in urban hydrology, and are lacking in many areas. We develop a high-resolution (15 min, 1 km^2) radar rainfall data set for Charlotte, North Carolina during the 2001-2010 period using the Hydro-NEXRAD system with radar reflectivity from the National Weather Service Weather Surveillance Radar 1988 Doppler weather radar located in Greer, South Carolina. A dense network of 71 rain gages is used for estimating and correcting radar rainfall biases. Radar rainfall estimates with daily mean field bias (MFB) correction accurately capture the spatial and temporal structure of extreme rainfall, but bias correction at finer timescales can improve cold-season and tropical cyclone rainfall estimates. Approximately 25 rain gages are sufficient to estimate daily MFB over an area of at least 2,500 km^2, suggesting that robust bias correction is feasible in many urban areas. Conditional (rain-rate dependent) bias can be removed, but at the expense of other performance criteria such as mean square error. Hydro-NEXRAD radar rainfall estimates are also compared with the coarser resolution (hourly, 16 km^2) Stage IV operational rainfall product. Stage IV is adequate for flood water balance studies but is insufficient for applications such as urban flood modeling, in which the temporal and spatial scales of relevant hydrologic processes are short. We recommend the increased use of high-resolution radar rainfall fields in urban hydrology.

(KEY TERMS: precipitation; radar; rain gages; urban hydrology; NEXRAD; rain gage networks; rainfall-runoff; spatial and temporal resolution.)

Wright, Daniel B., James A. Smith, Gabriele Villarini, and Mary Lynn Baeck, 2013. Long-Term High-Resolution Radar Rainfall Fields for Urban Hydrology. *Journal of the American Water Resources Association* (JAWRA) 50(3): 713-734. DOI: 10.1111/jawr.12139

INTRODUCTION

The National Weather Service (NWS) Next-Generation Radar (NEXRAD) (Heiss *et al.*, 1990) network has provided high-resolution rainfall fields over the conterminous United States (U.S.) for more than 10 years. These long-term rainfall records, when subject to proper quality control and bias correction, represent a valuable resource for hydrologists and engineers, particularly in urban settings, where spatially continuous rainfall estimates at high spatial and temporal resolutions are necessary (see Schilling, 1991; Smith *et al.*, 2002; Berne *et al.*, 2004b; Creutin *et al.*, 2009; Emmanuel *et al.*, 2012; Looper and Vieux, 2012) and where dense rain gage networks can be difficult and expensive to install and maintain.

Long-term (10-year) bias-corrected radar rainfall fields at the 15-min temporal resolution and 1-km^2 spatial resolution have been developed for several metropolitan areas in the U.S. with the Hydro-NEXRAD

[1]Paper No. JAWRA-12-0213-P of the *Journal of the American Water Resources Association* (JAWRA). Received September 17, 2012; accepted August 28, 2013. **Discussions are open until six months from print publication**.

[2]Doctoral Candidate (Wright), Professor (Smith), and Hydrometeorology Programmer (Baeck), Department of Civil and Environmental Engineering, Princeton University, E208 Engineering Quad, Princeton, New Jersey 08544; and Assistant Professor (Villarini), Department of Civil and Environmental Engineering, University of Iowa, Iowa City, Iowa 52242 (E-Mail/Wright: danielb.wright@gmail.com).

processing system (Krajewski *et al.*, 2010b) and have been used to examine such diverse topics as urban modification of rainfall (Smith *et al.*, 2012; Wright *et al.*, 2012; Yang *et al.*, 2013), storm event hydrologic response (Wright *et al.*, 2012; Smith *et al.*, 2013; Yang *et al.*, 2013), and frequency analysis of extreme rainfall (Wright *et al.*, 2013; see Overeem *et al.*, 2009 for related work in the Netherlands) and flooding (D.B. Wright, J.A. Smith, and M.L. Baeck, 2013, manuscript in revision). The accuracy of these datasets and the effectiveness of the bias-correction procedures have not been thoroughly demonstrated, however. In addition, the utility of these bias-corrected Hydro-NEXRAD fields has not been compared to that of commonly used operational radar- or multi-sensor rainfall estimates.

More generally, radar rainfall fields have been used in a variety of urban flood studies (e.g., Bedient *et al.*, 2000; Smith *et al.*, 2002, 2005a, 2007; Vieux and Bedient, 2004; Vieux and Vieux, 2005; Sharif *et al.*, 2010a; Villarini *et al.*, 2010, 2013; Wright *et al.*, 2012), but have yet to achieve wide acceptance by researchers or practicing engineers due to a long-standing lack of familiarity with their use or a lack of confidence in their accuracy (Wilson and Brandes, 1979; Einfalt *et al.*, 2004).

This study addresses these gaps, and in doing so, demonstrates the strengths and weaknesses of long records of high-resolution bias-corrected radar rainfall fields relative to other rainfall datasets (namely, rain gages and operational multi-sensor rainfall products). We focus on the spatial and temporal scales that are relevant for urban hydrology and present several potential applications. These scales depend on location and on the relevant physical processes, but are generally on the order of several minutes to several hours and tens of meters to tens of kilometers (see Schilling, 1991 and Berne *et al.*, 2004b for more detailed discussion of length and time scales in urban hydrology).

Any comparison of radar pixel observations to rain gage accumulations will reflect not just measurement errors but also the different spatial sampling properties of the two instruments (see, e.g., Anagnostou *et al.*, 1999; Ciach and Krajewski, 1999; Villarini and Krajewski, 2009). These errors are particularly evident for short aggregation periods and for larger radar pixels. Radar measures reflectivity, or the amount of backscattered radiation from a radar beam, in a volume of air of up to several cubic kilometers. Backscattering will occur due to liquid or frozen precipitation as well as ground obstructions and atmospheric phenomena. Rain gages, meanwhile, measure ground surface-level rainfall over an area of approximately 0.1 m^2. Both instruments may exhibit measurement biases. In this study, we focus only on radar bias.

Two types of radar rainfall biases and corresponding correction procedures are examined in this study. The first type is mean field bias (MFB) (Smith and Krajewski, 1991; Seo, 1998; Seo *et al.*, 1999) which does not vary in space and arises due to variability in Z-R relationships (discussed further in the following section) and radar calibration errors (Villarini and Krajewski, 2010b). The second type is called conditional bias (CB) (see Ciach *et al.*, 2000, 2007; Villarini *et al.*, 2008b). A general overview of radar rainfall estimation can be found in Krajewski and Smith (2002), while error sources in radar rainfall estimates are discussed in detail in Villarini and Krajewski (2010b) and Krajewski *et al.* (2010a). Interested readers are pointed to studies that address spatio-temporal uncertainties in radar rainfall estimates (e.g., Ciach and Krajewski, 1999; Germann *et al.*, 2009; Villarini and Krajewski, 2009, 2010a; Kirstetter *et al.*, 2010) and a number of studies that examine the propagation of radar rainfall uncertainties in hydrologic models (e.g., Borga, 2002; Hossain *et al.*, 2004; Gourley and Vieux, 2005; Borga *et al.*, 2006; Habib *et al.*, 2008; Germann *et al.*, 2009; Schröter *et al.*, 2011; Vieux and Imgarten, 2012).

This study focuses on the following topics:

1. Long-term (10-year) high-resolution (15 min, 1 km^2) bias-corrected Hydro-NEXRAD radar rainfall datasets are evaluated and compared against observations from a dense urban rain gage network for the Charlotte, North Carolina metropolitan region. Error statistics associated with a biased (henceforth referred to as "uncorrected") dataset and two MFB-corrected datasets (corrected at daily and hourly timescales) are examined for accumulation periods ranging from 15 min to 12 h for the warm (April-September) and cold (October-March) seasons.
2. Conditional bias for a range of accumulation periods relevant to urban hydrology for the warm (April-September) and cold (October-March) seasons is examined. Some comments are made about the challenges associated with the use of CB correction in hydrologic practice.
3. The accuracy and utility of the coarser-resolution (hourly, 16 km^2) Stage IV operational rainfall product from the National Center for Environmental Prediction (NCEP) (see http://www.emc.ncep.noaa.gov/mmb/ylin/pcpanl/stage4 for more information) is discussed with respect to Hydro-NEXRAD radar datasets.
4. The impact of the number of rain gages on MFB estimation is evaluated. Many studies have examined the effects of rain gage number, density, and configuration on direct measurement of rainfall (see, e.g., Thol, 1972; Rodriguez-Iturbe

and Mejia, 1974; Moore *et al.*, 2000; Villarini *et al.*, 2008a), but we are not aware of any studies that have examined rain gage networks specifically for radar MFB bias correction.

5. Estimates of heavy rainfall from bias-corrected Hydro-NEXRAD datasets, dense rain gage networks, and the Stage IV operational rainfall product are examined for several urban hydrologic applications across a range of spatial and temporal scales. Applications include the characterization of the regional climatology (spatial variability of long-term rainfall patterns) of warm season rainfall, examination of the flood water balance for a set of storms, and in-depth examination of several extreme tropical and nontropical storms.

DATA AND METHODS

The Charlotte metropolitan area is an ideal setting for flood hydrology research due to the available data resources and the variety of recent flood-producing tropical storms and organized thunderstorm systems. The Blue Ridge Mountains to the west affect storm initiation and evolution across the region (Weisman, 1990a, b; Murphy and Konrad, 2005) while local topographic relief is minimal. Radar estimation of rainfall for characterization of several extreme floods in Charlotte has been examined in Smith *et al.* (2002), Turner-Gillespie *et al.* (2003), and Villarini *et al.* (2010). Two NWS Weather Surveillance Radar 1988 Doppler (WSR-88D) radars, Greer, South Carolina (KGSP) and Columbia, South Carolina (KCAE) cover the Charlotte area. The KCAE radar is located such that beam blockage over the Charlotte area is a major problem (see Villarini and Krajewski, 2010b for further discussion of beam blockage). The KGSP radar has been selected for use in this study due to the lack of beam blockage and the favorable range (approximately 130 km; Figure 1, left panel) from the Charlotte area. Analyses indicate that range effects on radar rainfall estimation for the Charlotte metropolitan region are minimal (results not shown).

Radar rainfall estimates from the KGSP radar are bias-corrected using rain gage measurements from 71 5-min resolution gages of the Charlotte Raingage Network (CRN) (Figure 1, right panel) operated jointly by the U.S. Geological Survey (USGS) and Charlotte-Mecklenburg Storm Water

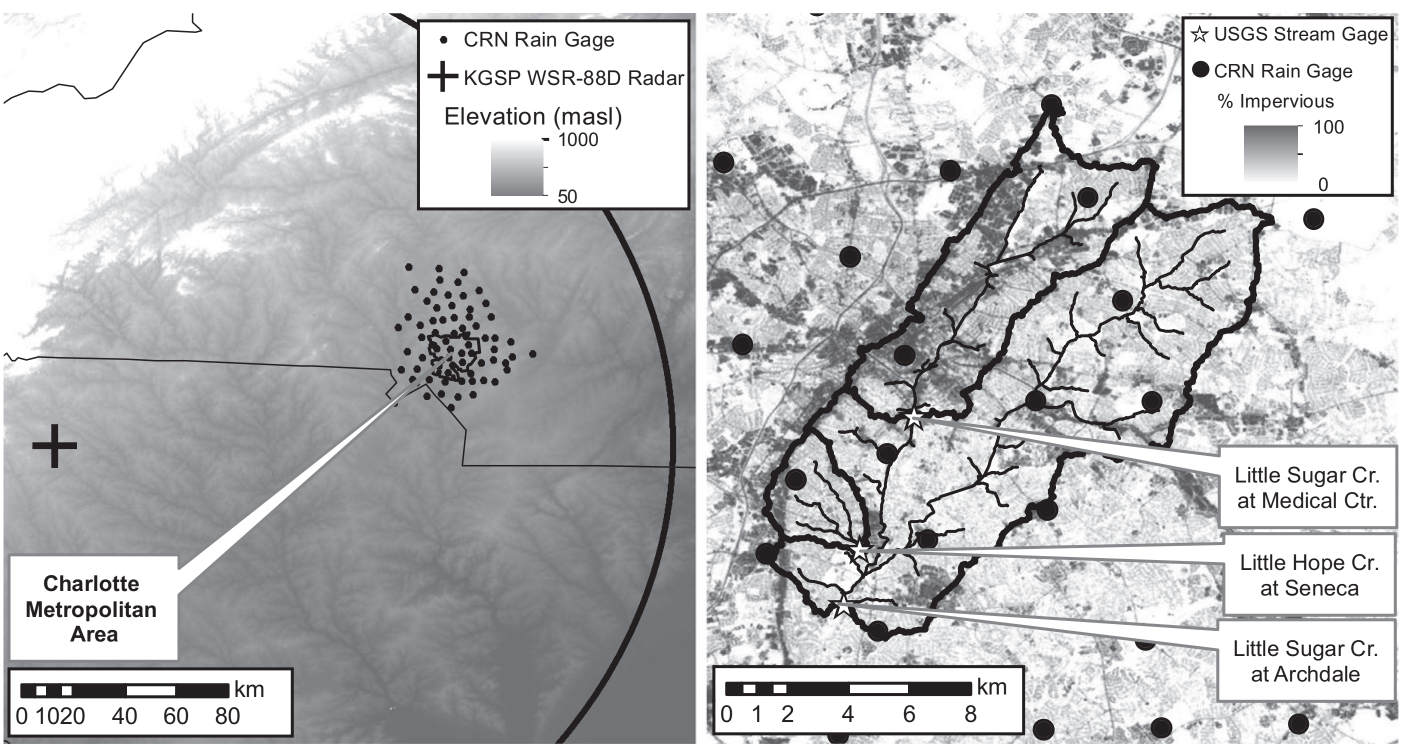

FIGURE 1. Study Region. Left panel: KGSP radar location, 200-km range envelope of the KGSP radar umbrella, state boundaries, regional topography, and the Charlotte metropolitan boundary. Right panel: Charlotte metropolitan area with the location of Charlotte Raingage Network (CRN) rain gages, U.S. Geological Survey (USGS) stream gages, and outlines of three subbasins of Little Sugar Creek.

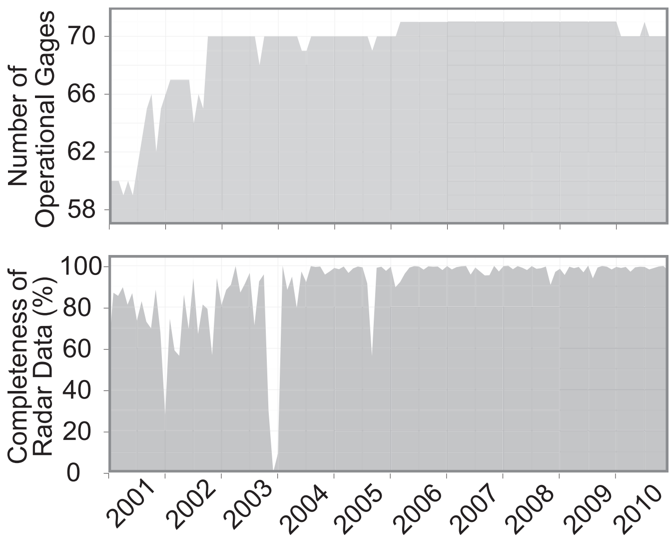

FIGURE 2. Top panel: Number of Charlotte Raingage Network Rain Gages Reporting and Properly Functioning by Month from 2001 to 2010. Bottom panel: Percent of KGSP 15-min radar periods available per month from 2001 to 2010.

Services. Most of these gages have been operational since at least 1995 and the network is subject to a high degree of quality control. The availability of contemporaneous radar and CRN rain gage observations is generally good for the 2001-2010 period (Figure 2). The CRN is one of the most dense and best maintained urban rain gage networks in the world and thus is valuable for radar validation (see, e.g., Villarini *et al.*, 2010).

The USGS also maintains a dense network of approximately 40 stream gages in the Charlotte metropolitan area. Three stream gages have been selected for detailed intercomparison of basin-scale radar and rain gage estimates of extreme rainfall and for examining relationships between rainfall and urban flood response at a variety of spatial and temporal scales. The three chosen gages delimit subcatchments of Little Sugar Creek, which drains much of central Charlotte (Figure 1, right panel). The subcatchments range in size from 6.7 to 110 km^2 and are highly urbanized (see Table 1). Streamflow data are available at a resolution of 15 min for the 2001-2010 study period.

The Hydro-NEXRAD processing system was developed specifically for the production of rainfall estimates for hydrologic applications, and converts three-dimensional polar coordinate volume scan reflectivity fields from NWS WSR-88D radars into two-dimensional Cartesian surface rainfall fields through a rainfall-reflectivity (Z-R) relationship of the form $R = aZ^b$, where R is rain rate in mm/h, and Z is the radar reflectivity factor in mm^6/m^3.

Two common parameterizations of the Z-R relationship are available for NEXRAD, the "standard," and a second that is occasionally used for tropical storm conditions (Fulton *et al.*, 1998). The choice of Z-R relationship can impart substantial differences on resulting radar rainfall estimates (see Smith *et al.*, 2005b), although these differences can be minimized through bias correction. We use the standard convective Z-R relationship (a = 0.017, b = 0.714), as well as a 53-decibel (dBZ) hail threshold and several standard quality control algorithms including the removal of anomalous propagation returns (Steiner and Smith, 2002), and hail detection and mitigation (Baeck and Smith, 1998; Fulton *et al.*, 1998).

We compute and compare MFB at two time scales: daily (12-12 Coordinated Universal Time [UTC]) and hourly. The MFB computation takes the form:

$$B_i = \frac{\sum_{S_i} G_{ij}}{\sum_{S_i} R_{ij}} \qquad (1)$$

where G_{ij} is the rainfall accumulation for gage j for time period i (in this study, the duration of i is 1 day or 1 h), R_{ij} is the rainfall accumulation for the radar pixel containing gage j for time period i, and S_i is the index of the rain gage stations for which both the rain gage and the radar report positive rainfall accumulations during time period i. Each 15-min radar rainfall field within time period i is then multiplied by the bias correction factor B_i. For time periods in which less than five gages reported positive rainfall, a bias value was computed from long-term seasonal rainfall totals (warm season: April-September, or cold season: October-March) by dividing the total seasonal gage-estimated rainfall by the total uncorrected radar-estimated rainfall, excluding tropical storms. The rainfall estimates from the two bias-correction time scales, as well as from the uncorrected Hydro-

TABLE 1. Land Surface Characteristics for Three Urban Study Watersheds.

Watershed/USGS Gage Name	USGS ID	Area (km^2)	2006 Urban Land Use (%)	2006 Impervious (%)	Slope (%)
Little Hope Cr. at Seneca	02146470	6.7	98	41	5.9
Little Sugar Cr. at Medical Ctr.	02146409	31	98	48	5
Little Sugar Cr. at Archdale	02146507	110	97	32	5.8

NEXRAD and the NCEP Stage IV multi-sensor product, are compared throughout this study.

The daily variant of the bias correction procedure is the same as that used in previous urban flood hydrology studies (Smith *et al.*, 2012, 2013; Wright *et al.*, 2012, 2013; D.B. Wright, J.A. Smith, and M.L. Baeck, 2013, manuscript in revision). Many rain gage networks in the U.S., including the Community Collaborative Rain, Hail and Snow Network (CoCoRaHS) (http://www.cocorahs.org/), much of the National Climate Data Center Network, and historical USGS rain gages report on a daily, rather than subdaily basis, so daily bias correction has the potential advantage of widespread applicability. Daily rain gage accumulations are also less subject to measurement errors than subdaily accumulations (see, e.g., Ciach, 2003), simplifying quality control prior to bias correction.

In this study, CB is modeled using the methodology presented in Villarini and Krajewski, 2009, which involves fitting a power law function of the form:

$$\hat{R}_T(t) = aR_R(t)^b \tag{2}$$

to the result of a locally weighted scatterplot smoothing (LOESS) (Cleveland, 1979) of the gage-radar pairs, where t is the aggregation period, a and b are empirical parameters, $R_R(t)$ is the radar pixel rainfall estimate, and $\hat{R}_T(t)$ is the estimate of true rainfall.

With the exception of the analyses of regional rainfall climatology, no range correction algorithms are used in this study. In other settings, particularly those more distant from the radar installation or that span a larger portion of the radar range envelope, range correction based on vertical profile of reflectivity corrections may be necessary (see, e.g., Andrieu and Creutin, 1995; Seo *et al.*, 2000; Vignal and Krajewski, 2001; Berne *et al.*, 2004a; Germann *et al.*, 2006; Bellon *et al.*, 2007; and Krajewski *et al.*, 2011).

Stage IV rainfall fields provide hourly multi-sensor rainfall estimates with a nominal spatial resolution of 16 km^2 over the conterminous U.S. Each of the twelve NWS River Forecast Centers (RFC) creates an hourly regional multi-sensor precipitation estimate (MPE) by merging NEXRAD radar and rain gage (and, in some cases, satellite-based) measurements which are then mosaicked into the nationwide Stage IV product in near-realtime at NCEP. Quality control for the rainfall estimates that form the MPE is not necessarily uniform and metadata is generally not available regarding the data and procedures that have been used for any particular time period or location. Stage IV has been used for hydrologic applications ranging from hydrologic modeling in the southwestern U.S. (e.g., Sharif *et al.*, 2010a, b; El Hassan *et al.*, 2012) to the characterization of tropical storm rainfall and flooding along the Atlantic coast (Villarini *et al.*, 2011). Several studies have focused on validating Stage IV rainfall estimates (e.g., Westcott *et al.*, 2008; Habib *et al.*, 2009; Cunha *et al.*, 2012). Its resolution is coarse compared to what is generally considered necessary for urban hydrology (Schilling, 1991; Smith *et al.*, 2002; Berne *et al.*, 2004b).

Rainfall associated with tropical cyclones is identified using the Hurricane database from the National Oceanographic and Atmospheric Administration (NOAA) National Hurricane Center (see Jarvinen *et al.*, 1984; Neumann *et al.*, 1993). Any rainfall occurring 12 h before to 12 h after a center of circulation passes within 500 km of Charlotte is classified as tropical in origin (see Hart and Evans, 2001; Kunkel *et al.*, 2011; and Villarini and Smith, 2010 for similar classification criteria for tropical rainfall).

BIAS-CORRECTION OF RADAR RAINFALL

Mean field bias correction performed at the daily and hourly scales significantly improves radar estimates of 15-min and 12-h rainfall accumulations compared with the uncorrected Hydro-NEXRAD (Figure 3). The effect of the 53 dBZ hail threshold is clearly evident in the uncorrected 15-min accumulations, imposing a maximum rainfall rate of approximately 100 mm/h (Figure 3, top-left panel). The extent of scatter is similar for both bias-corrected datasets and is significantly less than that of the uncorrected dataset. The effect of the hail cap is no longer apparent (Figure 3, center and right panels). The data are more highly scattered for 15-min accumulations than for 12-h accumulations since both gage and radar measurement errors tend to be less severe as observations are temporally aggregated (Habib *et al.*, 2001; Ciach, 2003).

Conditional bias is illustrated in Figure 3 by the dashed lines which show the results of LOESS regression. CB at the 15-min scale is similar for all three datasets but is greater for the uncorrected data than for either corrected dataset at the 12-h scale. For rainfall accumulation periods between 15 min and 12 h, scatter and CB decrease with increasing accumulation time, particularly for the two bias-corrected datasets (results not shown). MFB correction, therefore, significantly reduces CB, at least for long accumulation periods. These results are consistent with Villarini *et al.* (2010), who did not find any significant CB in storm total rainfall after MFB correction.

Error statistics are computed relative to co-located rain gage observations for warm- and cold-season

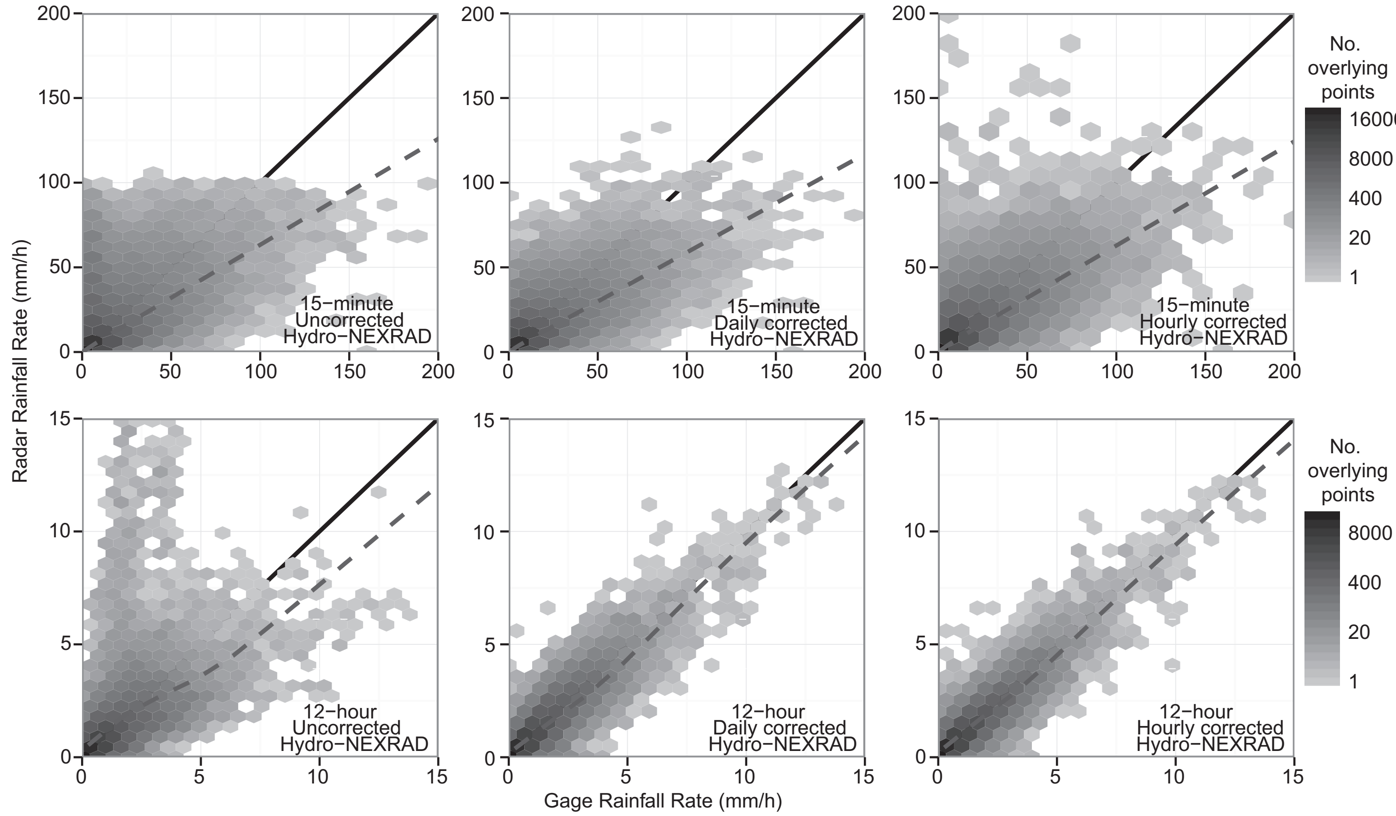

FIGURE 3. Comparison of Co-located Rain Gage and Radar-Estimated Rainfall Accumulations for the KGSP Radar for Uncorrected Radar (left panels), and Radar with Mean Field Bias Correction Done at the Daily (center panels) and Hourly Scales (right panels) for All Seasons for the 2001-2010 Period. Rainfall accumulations are shown at the 15-min (top panels) and 12-h (bottom panels) scales. Conditional bias is highlighted using a locally weighted scatterplot smoothing fit (dark gray dashed lines). Darker shading indicates a higher point density.

15-min, 1-h, 3-h, and 12-h time radar rainfall accumulations for the uncorrected and two MFB-corrected Hydro-NEXRAD datasets (Table 2). The Pearson correlation coefficient (r), root-mean-square error (RMSE), and mean absolute error (MAE) all improve substantially with bias correction. MFB correction performed at the hourly scale gives the best results at shorter accumulation periods, especially 1 h. At longer

TABLE 2. Error Statistics for 15-min, 1-h, 3-h, and 12-h Rainfall Accumulations for Uncorrected Radar Rainfall and Radar Rainfall with Mean Field Bias Correction at the Daily and Hourly Scales.

Season	Statistic	Uncorrected	Daily	Hourly	Uncorrected	Daily	Hourly
		15 min			1 h		
Warm	r	0.717	0.762	0.773	0.8	0.856	0.866
	RMSE (mm)	0.311	0.279	0.276	0.731	0.606	0.593
	MAE (mm)	0.026	0.023	0.022	0.087	0.071	0.067
Cold	r	0.459	0.673	0.688	0.546	0.777	0.81
	RMSE (mm)	0.282	0.172	0.165	0.821	0.436	0.381
	MAE (mm)	0.022	0.018	0.016	0.077	0.06	0.05
		3 h			12 h		
Warm	r	0.822	0.885	0.893	0.828	0.911	0.913
	RMSE (mm)	1.468	1.161	1.136	3.468	2.53	2.526
	MAE (mm)	0.237	0.183	0.173	0.873	0.612	0.606
Cold	r	0.59	0.843	0.864	0.595	0.899	0.889
	RMSE (mm)	2.012	0.906	0.791	6.171	2.02	1.998
	MAE (mm)	0.411	0.264	0.229	0.789	0.458	0.425

Note: RMSE, root-mean-square error; MAE, mean absolute error.

TABLE 3. Error Statistics for 1-, 3-, and 12-h Rainfall Accumulations for Stage IV Radar Data from 2002 to 2010.

Season	Statistic	1 h	3 h	12 h
Warm	r	0.809	0.851	0.884
	RMSE (mm)	0.733	1.403	3.115
	MAE (mm)	0.094	0.241	0.837
Cold	r	0.795	0.852	0.882
	RMSE (mm)	0.433	0.913	2.313
	MAE (mm)	0.064	0.167	0.568

Note: RMSE, root-mean-square error; MAE, mean absolute error.

accumulation periods, the accuracy of the two bias-corrected datasets converge. Correlation is generally higher for the warm season than for the cold season for all accumulation periods, particularly for the uncorrected dataset. This is likely due to bright band enhancement of radar reflectivity above the atmospheric freezing level or difficulty in discriminating between liquid and frozen precipitation with both gages and radar (Borga *et al.*, 2002; Rinehart, 2004; Hazenberg *et al.*, 2011). Post-bias correction RMSE and MAE are greater for the warm season than for the cold season for all accumulation periods due to higher rain rates during the summer months.

Error statistics are also computed for the NCEP Stage IV rainfall product for 1-, 3-, and 12-h accumulations (Table 3). During the warm season, Stage IV estimation errors are comparable to the uncorrected Hydro-NEXRAD. Stage IV performs better than the uncorrected Hydro-NEXRAD during the cold season. In no instance does the Stage IV perform as well as either bias corrected Hydro-NEXRAD dataset, although 1-h cold season accumulations are similar for Stage IV and bias-corrected Hydro-NEXRAD. It should be pointed out that Stage IV pixel accumulations are more likely than Hydro-NEXRAD pixel accumulations to deviate from co-located rain gage accumulations due to the coarser spatial resolution of Stage IV. This impact is likely to be more significant during the warm season due to the sharp spatial gradients that characterize summertime convective precipitation. That may explain some of the differences between the Stage IV and the bias-corrected Hydro-NEXRAD, as well as the fact that the uncorrected Hydro-NEXRAD performs comparably to the Stage IV during the warm season in spite of its substantial biases. It is unclear whether CRN gages are merged into the Stage IV estimates, but in general, the rain gage networks that are merged into Stage IV estimates are sparser than the CRN network, and may therefore underestimate spatially small convective rain cells.

Conditional bias can be removed by applying the CB correction shown in Equation (2) (Figure 4; see Table 4 for the power law parameters a and b used for CB correction), but at the expense of other performance criteria such as RMSE and MAE (note the error statistics and the increased scatter above the 1:1 line in Figure 4). This tradeoff between CB and other performance criteria is noted in Ciach *et al.* (2000), and occurs because MFB-corrected estimates are by definition unbiased with respect to a multiplicative factor. Whether or not to use CB correction in practice would depend, therefore, on the particular application: if the estimation of extreme rain rates is important, CB correction may be appropriate. For applications which require accurate estimation of rainfall depths over relatively long accumulation periods, CB correction is likely not desirable. No subsequent analyses in this study employ CB correction.

The spatial structure of rainfall estimates from the CRN network and corresponding MFB-corrected radar pixel estimates are examined at the 15-min scale. We calculate the spatial correlation by calculating the correlation between all 15-min gage/pixel accumulations that have a given separation distance d. The spatial correlation is somewhat lower for the rain gages than for the radar for both warm and cold seasons, likely due to differences in properties of spatial sampling and error properties of the two instruments (Figure 5). Warm season spatial correlation is lower than in the cold season, due to sharper spatial gradients in summertime convective rainfall.

The temporal structure of radar bias is examined by computing the autocorrelation of the sum of all positive rain gage measurements divided by the sum of all co-located uncorrected Hydro-NEXRAD radar pixel rainfall estimates at the 15-min scale (Figure 6, top panels). During the warm season, there is persistent autocorrelation until about the 9-h time lag, suggesting that MFB correction performed at time scales longer than 1 h is appropriate. Autocorrelation in 15-min bias is higher in the warm season than the cold season for separation lags up to approximately 9 h. This may be due to seasonal differences in atmospheric properties that affect the propagation of the radar beam or difficulties in determining precipitation phase during the cold season. The lack of multi-hour persistence in the autocorrelation of 15-min bias

TABLE 4. Power-Law Parameters for Conditional Bias Correction Procedure. The cold season is October-March, the warm season is April-September.

Season	Parameter	15 min	1 h	3 h	12 h
Warm	a	1.285	1.053	0.979	1.059
	b	1.088	1.072	1.063	1.015
Cold	a	1.219	0.956	0.964	0.952
	b	1.153	1.098	1.031	1.010

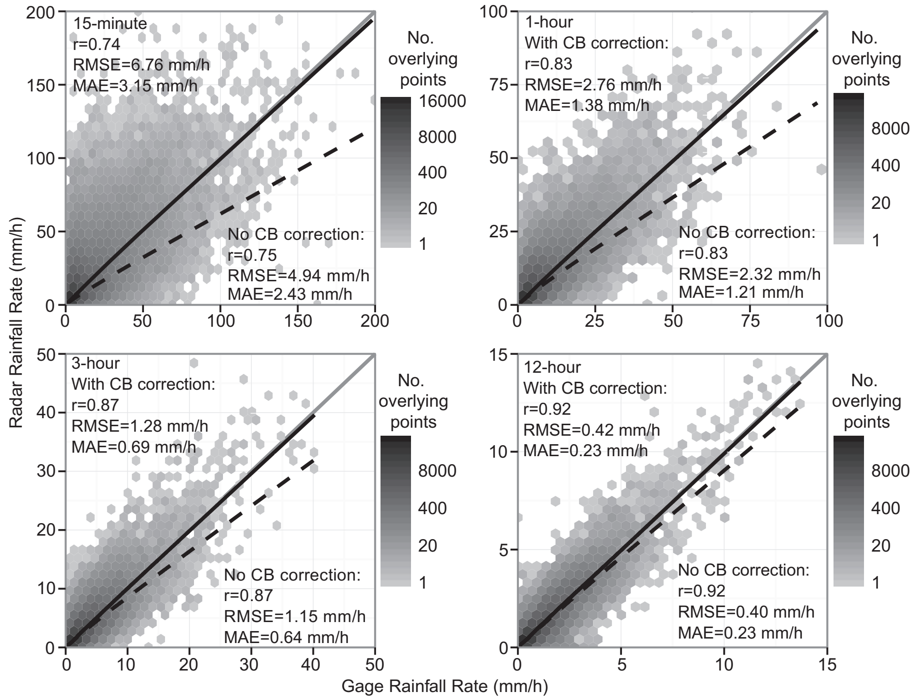

FIGURE 4. Demonstration of Conditional Bias (CB) Correction of *T*-Hour Radar Rainfall Estimates. Error statistics with and without CB correction are shown. Shading represents relative density of scatter pairs after mean field and CB correction. Locally weighted scatterplot smoothing has been done on mean field bias corrected Hydro-NEXRAD radar data prior to CB correction (dashed lines) and after CB correction (solid lines). Top left panel: 15-min scale. Top right: 1-h scale. Bottom left: 3-h scale. Bottom right: 12-h scale. RMSE, root-mean-square error; MAE, mean absolute error.

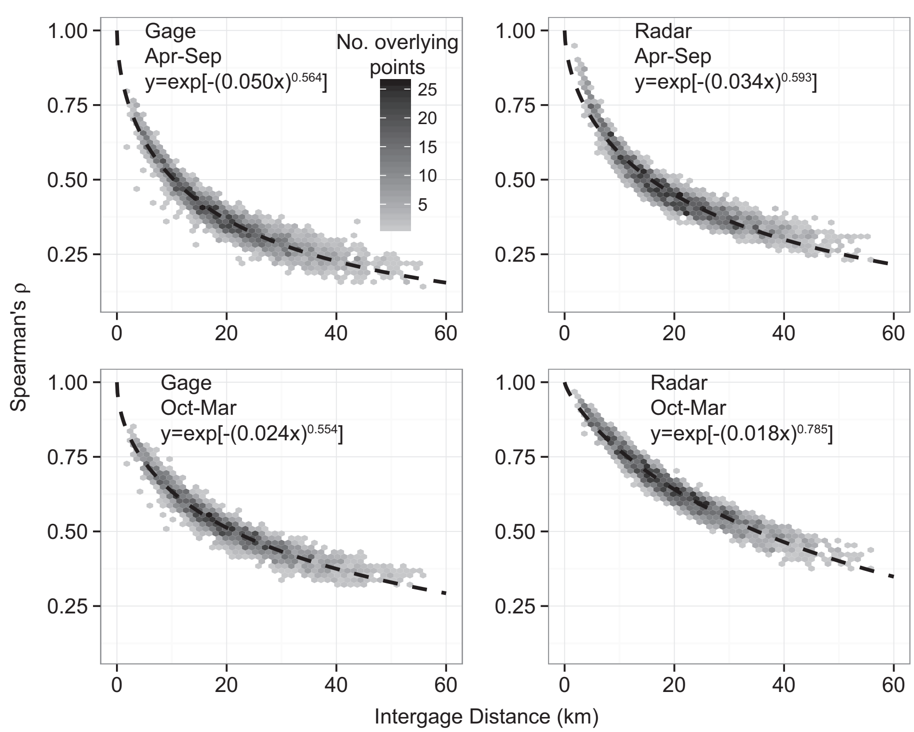

FIGURE 5. Comparison of Spatial Correlation of Rain Gage Accumulations (left panels) and Corresponding Hydro-NEXRAD with Daily-Scale Mean Field Bias Correction (right panels) at the 15-Min Time Scale for the Warm Season (April-September, top panels) and the Cold Season (October-March, bottom panels). Dashed lines represent the results of nonlinear least squares regression fits to power law functions.

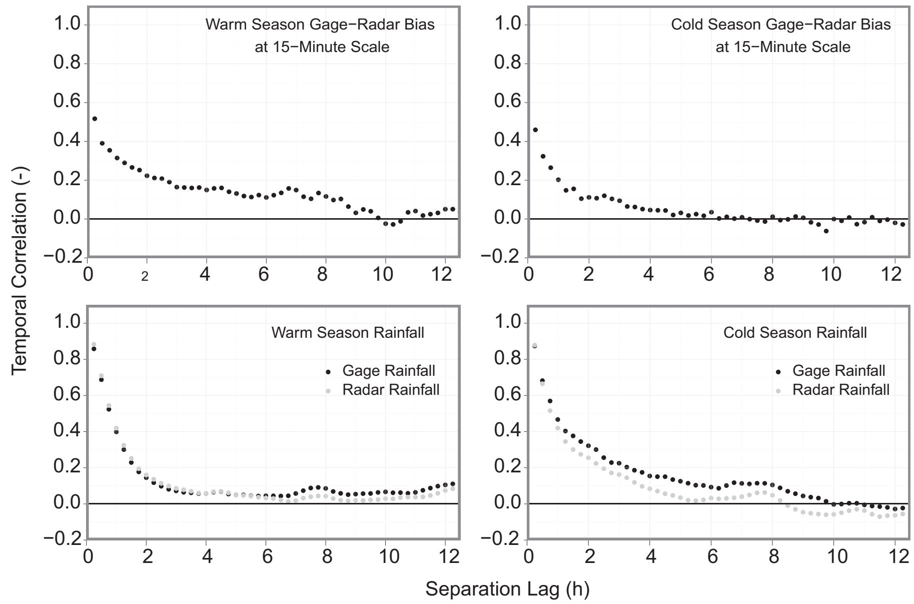

FIGURE 6. Autocorrelation in 15-Min Bias (sum of all positive gage accumulations divided by sum of corresponding radar pixel accumulations) Prior to Mean Field Bias (MFB) and Conditional Bias (CB) Correction of Radar Rainfall for the Warm Season (April-September, top left) and for the Cold Season (October-March, top right). Autocorrelation of 15-min rain gage and radar-estimated rainfall (the sum of all positive gage accumulations and the sum of corresponding radar pixel accumulations, respectively) after MFB and CB correction for April-September (bottom left) and October-March (bottom right).

during the cold season corroborates the error statistics in Table 2, which show that MFB correction at the hourly, rather than daily, scale yields greater improvement over bias-correction at the daily scale during the cold season compared with the warm season.

We also examine the temporal structure of radar and rain gage rainfall estimates, computed as the autocorrelation of the mean of all positive 15-min gage accumulations and of corresponding daily MFB-corrected radar accumulations (Figure 6, bottom panels). Temporal correlation of rainfall is lower in the warm season than in the cold season, again due to sharper spatial gradients in summertime convective rainfall. The temporal correlation structure of rainfall shows the inverse relationship (lower in the warm season, higher in the cold season) of that of radar bias.

RAIN GAGE NETWORKS FOR BIAS CORRECTION

Villarini *et al.* (2008a) demonstrate that accurate direct estimation of rainfall at high spatial and temporal resolution using rain gages requires very high gage densities. Most urban settings in the U.S. and elsewhere lack the high number of rain gages that are available in the Charlotte metropolitan area through the CRN network (71 gages, or approximately one gage per 35 km^2). The NEXRAD radar network, however, provides high-resolution rainfall estimates for all major urban areas in the conterminous U.S. Fewer gages are necessary for MFB estimation than for the direct high-resolution estimation of rainfall. It is useful, therefore, to examine the effect that the number of available gages has on the estimation of MFB.

We perform daily MFB correction using all *n-choose-k* combinations of 1, 5, 10, 25, and 50 CRN gages. We then compute the daily RMSE and MAE at the daily scale between the bias-corrected radar pixel accumulations and co-located rain gage accumulations and compare these error statistics to those from bias correction based on the entire 71-gage CRN network (Figure 7). Daily RMSE and MAE decreases exponentially from about 4.70 and 1.35 mm, respectively to about 3.60 and 1.60 mm as the number of gages used in bias estimation increases from 1 to 25. For more than 25 gages, improvement in RMSE and MAE is negligible. We do not examine the optimal geometric arrangement of gages; however, boxplots in Figure 7 consider all possible configurations and thus bound the possible range of errors for a given number of rain gages.

A network of 25 rain gages is sufficient to accurately estimate and correct for MFB at the spatial extent of the CRN rain gage network (approximately 2,500 km^2). This is comparable to gage densities in

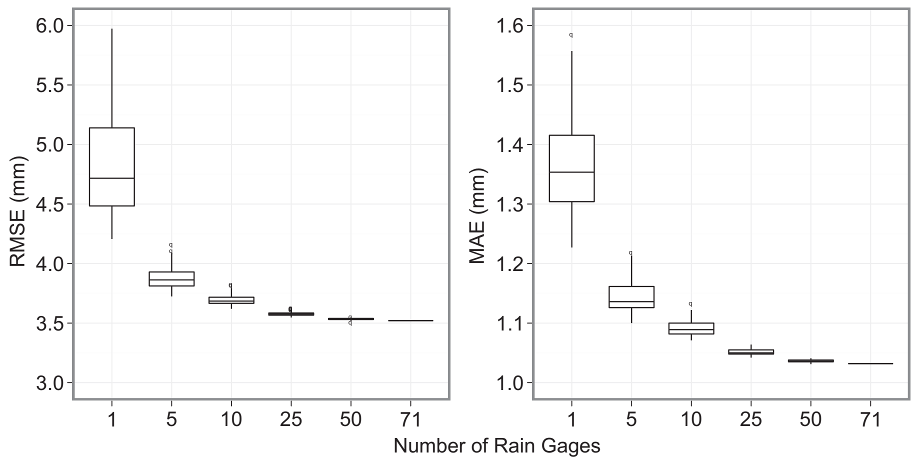

FIGURE 7. Error Statistics for Radar-Estimated Daily Rainfall Accumulations Based on n RainGages for Mean Field Bias (MFB) Correction. All *n-choose-k* combinations of rain gages are used for the MFB correction. Root-mean-square error (RMSE) (left panel) and mean absolute error (MAE) (right panel) are computed based on the difference between the sum of bias-corrected radar rainfall and gage-estimated rainfall at all 71 Charlotte Raingage Network gage locations. The box denotes the lower and upper quartiles, whiskers indicate the extent of the 1.5 interquartile range (IQR), and points indicate values beyond the 1.5 IQR.

many urban areas in the U.S. and elsewhere, suggesting that MFB correction of radar rainfall is feasible in many settings. We suggest, however, that more detailed studies should be conducted to assess the generalization of these conclusions to other settings and to examine over what spatial scales MFB correction is accurate.

RADAR-DERIVED RAINFALL CLIMATOLOGY

Long-term bias-corrected radar rainfall datasets can be used to examine regional rainfall patterns (see Overeem *et al.*, 2009; Smith *et al.*, 2012; Wright *et al.*, 2012). In this study, mean June-July-August (JJA) rainfall and mean number of JJA heavy rain (rainfall exceeding 25 mm) days are calculated over the region surrounding the Charlotte metropolitan area for the 2001-2010 period (Figure 8). Regional analyses require careful consideration of the effects of range from the radar on rainfall estimates. In this section, the effects of long-term range-dependent bias for both quantities were removed for this analysis by separating the radar domain into concentric range rings, computing the mean quantity for each ring, and then multiplying each cell in the radar domain by the ratio of its range ring mean quantity to the radar domain mean quantity. In addition, the

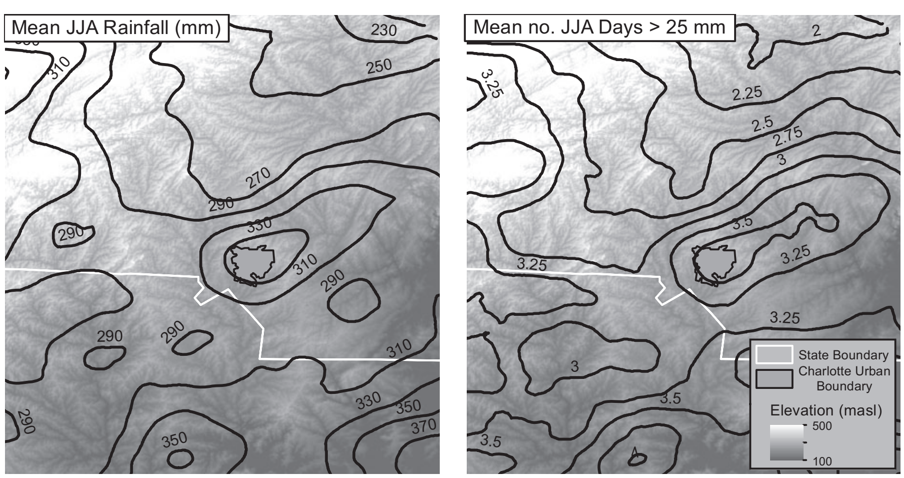

FIGURE 8. Left panel: Mean 2001-2010 June-July-August (JJA) Rainfall Derived from Hydro-NEXRAD Radar Rainfall Fields that Have Been Mean Field Bias Corrected at the Daily Scale. Right panel: Mean 2001-2010 number of JJA days with rainfall greater than 25 mm derived from bias-corrected radar rainfall fields. Grey area shows the Charlotte metropolitan area.

effect of missing records on seasonal rainfall means was addressed by computing a seasonal mean cell-by-cell from available records and then multiplying it by the ratio of the total number of 15-min periods in the season to the number of available 15-min radar fields.

There is a clear local maximum in both mean rainfall and mean number of heavy rain days within and downwind (northeast) of the city. This downwind rainfall maximum is consistent with observations using a variety of instruments in other urban areas (see, e.g., St. Louis, Missouri: Changnon *et al.*, 1971; Changnon, 1979; Atlanta, Georgia: Diem and Mote, 2005; Diem, 2008; Mote *et al.*, 2007; Shepherd *et al.*, 2002; Rose *et al.*, 2008; and Wright *et al.*, 2012; and Baltimore, Maryland: Smith *et al.*, 2012). It has been suggested that this downwind rainfall maximum can be attributed to urban heat island effects on circulation (e.g., Huff and Vogel, 1978; Hjelmfelt, 1982; Bornstein and Lin, 2000; Thielen *et al.*, 2000) and on urban roughness effects on low-level moisture convergence (e.g., Huff and Vogel, 1978; Hjelmfelt, 1982).

Analysis of regional rainfall patterns and urban rainfall modification using rain gage networks is difficult due to the limited spatial extent or limited gage density of most networks (see, e.g., Diem and Mote, 2005). The CRN network covers only the Charlotte metropolitan area, and there are only approximately 40 daily Global Historical Climatology Network rain gages within the 40,000 km^2 domain shown in Figure 8. Previous studies of urban enhancement of precipitation in Baltimore (Ntelekos *et al.*, 2007) and St. Louis (Huff and Vogel, 1978) have shown that regional topography can play an important role on precipitation in urban areas. Future urban rainfall studies should address topographic impacts, and long-term bias-corrected radar rainfall fields can provide a useful tool for evaluating such storm motion and evolution in ways that would not be possible using only rain gage observations (Wright *et al.*, 2012).

RAINFALL-RUNOFF RESPONSE

In this section we examine the utility of different rainfall datasets for urban rainfall-runoff and flood water balance studies in Charlotte. Rainfall-runoff response is examined by developing a sample of flood events at each station based on a peak discharge threshold. The threshold is selected to extract an average of five flood events per year from 2001 to 2010 USGS instantaneous discharge records for the three study watersheds, leading to a population of 50 flood peaks per watershed. Once a peak is selected, no other peak occurring in a 48-h period centered on the time of the selected peak can be included, ensuring that events with multiple peaks are not double counted. Fifteen-minute basin-averaged rainfall time series are generated using Hydro-NEXRAD rainfall fields that have been MFB corrected at the daily scale and at the hourly scale. Similar peaks-over-threshold analyses using long-term Hydro-NEXRAD datasets in Atlanta and Baltimore are shown in Wright *et al.* (2012) and Smith *et al.* (2013), respectively. In addition, basin-averaged rainfall time series are generated from the CRN using inverse distance weighting (IDW) interpolation with 15-min time resolution, and from the Stage IV multi-sensor radar rainfall product at hourly resolution.

Table 5 shows the median peak discharge per unit area and its variability as well as the median response time and its variability based on each of the four basin-averaged rainfall time series for each of the three study watersheds. We define response time as the time elapsed between the time of occurrence of the centroid of maximum 6-h rainfall and the time of peak discharge. The timing of the maximum 6-h rainfall, and thus the response time, can vary depending on the rainfall dataset being considered. Variability is represented by the dimensionless coefficient of variation (CV), which is the sample standard deviation divided by the sample mean. The magnitude and variability of peak discharge per unit area decreases with increasing area. Interestingly, all four rainfall data-

TABLE 5. Variability in Median Peak Discharge and Response Time (elapsed time between the occurrence of the rainfall centroid of the 6-h maximum rainfall and the time of maximum discharge) for Peaks-Over-Threshold Events. Quantities in parentheses are dimensionless coefficients of variation (standard deviation divided by mean).

Watershed	Median Peak Discharge ($m^3/s/km^2$)	Median Response Time (h)			
		Daily Correction	Hourly Correction	CRN	Stage IV
Little Hope Cr. at Seneca	2.44 (0.69)	0.79 (1.42)	0.84 (1.43)	0.85 (1.22)	1.08 (1.22)
Little Sugar Cr. at Medical Ctr.	1.91 (0.35)	0.72 (1.59)	0.64 (1.61)	0.67 (1.58)	1.08 (1.17)
Little Sugar Cr. at Archdale	1.17 (0.43)	1.82 (0.69)	1.72 (0.75)	1.79 (0.47)	2.16 (0.75)

Note: CRN, Charlotte Raingage Network.

sets show that the median response time for Little Sugar Creek at Medical Center is equal to (Stage IV) or less than (all other datasets) the median response time for Little Hope Creek, despite being larger (31 and 6.7 km^2, respectively). This is likely because Little Sugar Creek at Medical Center has more impervious area (48% compared with 32% for the other two study basins) and much of its urbanization is situated close to the basin outlet. The variability of response time based on three of the rainfall datasets (excluding Stage IV) is higher for Little Sugar Creek at Medical Center than for Little Hope Creek, pointing to the importance of the spatial distribution of urban land cover (see Meierdiercks *et al.*, 2010 and Wright *et al.*, 2012), as well as the spatio-temporal distribution of rainfall in controlling the variability of flood response. Response times based on the Stage IV data are longer than for the other datasets for all three watersheds due to its coarser temporal resolution (hourly rather than 15-min). This suggests that the resolution of the Stage IV data is inadequate for applications in which precise timing is required and the temporal scales of the runoff and flood-generating processes are less than several hours.

We also examine rainfall-runoff response in terms of runoff ratio, which is defined as the percentage of rainfall that leaves the basin as discharge. For each of the 50 storms from each basin, we compute 1-, 3-, 6-, and 12-h maximum rainfall and runoff depths and the associated runoff ratios using each of the four rainfall datasets. From these values, we then compute the median 1-, 3-, 6-, and 12-h maximum rainfall and runoff depths and median runoff ratios as well as the CVs (Table 6). Rainfall depths and runoff ratios show little difference between the Hydro-NEXRAD datasets bias-corrected at daily and hourly scales, suggesting that for the urban flood water balance studies like those presented in Wright *et al.* (2012) and Smith *et al.* (2013), MFB estimation and correction at time scales finer than daily may be unnecessary.

Stage IV median 1-h maximum rainfall depths are lower than the other datasets for all three basins, likely because the hourly resolution of the Stage IV does not capture extreme short-duration rain rates. For longer accumulation periods the differences in rainfall depths between different datasets are small. The underestimation of 1-h rainfall depth leads to high median 1-h runoff ratios compared with the other datasets. It is likely that runoff production in hydrologic models that employ infiltration schemes that are tied directly to rain rate (such as Green-Ampt infiltration) would be adversely affected by the coarse resolution of Stage IV rainfall estimates. This would be especially true for small urban basins where response times and flow paths are short and runoff production is predominantly Hortonian (surface runoff that occurs due to rainfall rates exceeding soil infiltration rates). Agreement between the Hydro-NEXRAD and Stage IV datasets for time periods greater than 1 h suggests that Stage IV is adequate for estimating rainfall depth and flood water balance computations for larger basins where the time scales of runoff production and channel processes are long relative to the resolution of the rainfall estimates.

The median 1-h maximum rainfall depth for Little Hope Creek calculated from the CRN dataset is higher (22.7 mm) than the median depths for the two Hydro-NEXRAD datasets (18.6 mm for daily bias correction; 19.6 mm for hourly bias correction). CRN rainfall depths tend to be greater than the other datasets in Little Hope Creek for longer accumulation periods, although the relative difference is less than at the 1-h scale. This may be due the presence of CB in radar estimates, which is more prevalent for shorter accumulation periods. However, there is little evidence of underestimation by the bias-corrected radar rainfall for the larger basins, perhaps because the overall rain rates are lower, or because CB decreases with increasing averaging area. An alternate explanation is the poor rain gage coverage in Little Hope Creek. There is only one rain gage located within the basin, on its western boundary (see Figure 1, right panel), and so the IDW interpolation routine may not properly capture the sharp spatial gradients in warm season convective rainfall that would comprise much of the peaks-over-threshold population for that watershed. This question could be addressed by examining co-located radar rainfall estimates and very dense rain gage observations, but is not possible given the gage density in Charlotte.

The variability in rainfall depths in Little Hope Creek is lower for the interpolated gage dataset than for the radar datasets, possibly due to poor gage coverage in the basin. Differences in rainfall depth variability between the CRN data and the radar-based data are less significant for the larger basins, although there is still a tendency for the CRN rainfall depths to be less variable than the radar rainfall depths. It is possible that more sophisticated interpolation methods (see, e.g., Seo, 1998) could compensate for limited gage density and yield more physically realistic results, but these methods necessarily introduce assumptions about spatial and/or temporal rainfall structure that may in reality vary significantly by season or by storm.

EXTREME STORM CASE STUDIES

We examine six extreme rainfall events that produced significant flooding in Charlotte to compare

TABLE 6. Median Flood Water Balance Components for Peaks-Over-Threshold Data Using Four Precipitation Datasets for Three Study Watersheds. Quantities in parentheses are dimensionless coefficients of variation (standard deviation divided by mean).

Watershed	1-h Rainfall (mm)	1-h Discharge (mm)	Runoff Ratio (%)	3-h Rainfall (mm)	3-h Discharge (mm)	Runoff Ratio (%)	6-h Rainfall (mm)	6-h Discharge (mm)	Runoff Ratio (%)	12-h Rainfall (mm)	12-h Discharge (mm)	Runoff Ratio (%)
Hydro-NEXRAD with daily mean field bias correction												
L. Hope Cr. at Seneca	18.6 (0.52)	5.3 (0.76)	27 (0.50)	29.7 (0.58)	8.3 (0.63)	27 (0.50)	35.9 (0.57)	10.0 (0.60)	28 (0.43)	42.5 (0.61)	11.2 (0.63)	27 (0.44)
L. Sugar Cr. at Medic. Ctr.	20.0 (0.40)	5.2 (0.39)	28 (0.35)	31.1 (0.45)	12.4 (0.39)	40 (0.30)	36.2 (0.45)	15.7 (0.41)	41 (0.31)	41.7 (0.54)	17.5 (0.45)	43 (0.31)
L. Sugar Cr. at Archdale	17.9 (0.46)	4.0 (0.45)	23 (0.45)	28.8 (0.45)	9.8 (0.46)	32 (0.40)	36.3 (0.43)	13.9 (0.54)	35 (0.38)	44.4 (0.52)	15.9 (0.59)	36 (0.36)
Hydro-NEXRAD with hourly mean field bias correction												
L. Hope Cr. at Seneca	19.6 (0.53)	5.3 (0.76)	25 (0.56)	28.5 (0.58)	8.3 (0.63)	27 (0.44)	32.9 (0.59)	10.0 (0.60)	27 (0.42)	43.4 (0.64)	11.2 (0.63)	27 (0.54)
L. Sugar Cr. at Medic. Ctr.	21.9 (0.42)	5.2 (0.39)	26 (0.39)	31.7 (0.43)	12.4 (0.39)	41 (0.29)	37.9 (0.44)	15.7 (0.41)	42 (0.31)	43.8 (0.53)	17.5 (0.45)	43 (0.33)
L. Sugar Cr. at Archdale	19.5 (0.49)	4.0 (0.45)	24 (0.60)	27.6 (0.46)	9.8 (0.46)	32 (0.45)	34.5 (0.44)	13.9 (0.54)	34 (0.43)	44.4 (0.53)	15.9 (0.59)	35 (0.42)
IDW-interpolated CRN rain gage network												
L. Hope Cr. at Seneca	22.7 (0.48)	5.3 (0.76)	24 (0.60)	30.4 (0.54)	8.3 (0.63)	26 (0.48)	33.2 (0.51)	10.0 (0.60)	27 (0.42)	44.6 (0.50)	11.2 (0.63)	24 (0.42)
L. Sugar Cr. at Medic. Ctr.	21.3 (0.41)	5.2 (0.39)	28 (0.39)	33.5 (0.42)	12.4 (0.39)	40 (0.27)	38.8 (0.41)	15.7 (0.41)	43 (0.27)	44.5 (0.47)	17.5 (0.45)	40 (0.28)
L. Sugar Cr. at Archdale	19.6 (0.49)	4.0 (0.45)	24 (0.52)	30.3 (0.42)	9.8 (0.46)	33 (0.38)	38.0 (0.38)	13.9 (0.54)	37 (0.38)	45.3 (0.45)	15.9 (0.59)	36 (0.36)
NCEP Stage IV multisensor product												
L. Hope Cr. at Seneca	17.3 (0.66)	5.3 (0.76)	33 (0.49)	26.8 (0.61)	8.3 (0.63)	33 (0.54)	34.7 (0.58)	10.0 (0.60)	30 (0.52)	43.5 (0.57)	11.2 (0.63)	27 (0.54)
L. Sugar Cr. at Medic. Ctr.	18.8 (0.45)	5.2 (0.39)	34 (0.38)	31.8 (0.45)	12.4 (0.39)	43 (0.31)	38.5 (0.48)	15.7 (0.41)	40 (0.36)	42.1 (0.58)	17.5 (0.45)	41 (0.38)
L. Sugar Cr. at Archdale	15.2 (0.59)	4.0 (0.45)	28 (0.51)	28.6 (0.52)	9.8 (0.46)	33 (0.44)	35.7 (0.50)	13.9 (0.54)	37 (0.42)	48.4 (0.58)	15.9 (0.59)	37 (0.43)

Note: IDW, inverse distance weighting; CRN, Charlotte Raingage Network; NCEP, National Center for Environmental Prediction.

flood-producing rainfall from tropical storms to that from nontropical storms, and to compare estimates of extreme rainfall from bias-corrected Hydro-NEXRAD, the CRN gage network, and Stage IV. Three are tropical storms: Tropical Storm Fay (26-27 August 2008), Hurricane Jeanne (27-28 September 2004), and Hurricane Frances (7-8 September 2004), and three are warm-season convective systems: 7-8 June 2003, 15-16 August 2006, and 4-6 May 2009.

Scatterplots of 1- and 12-h radar *vs*. gage accumulations for the tropical cyclones illustrate severe underestimation of extreme rainfall during tropical events in the uncorrected Hydro-NEXRAD data (Figure 9, left panels). Using the tropical *Z-R* relationship

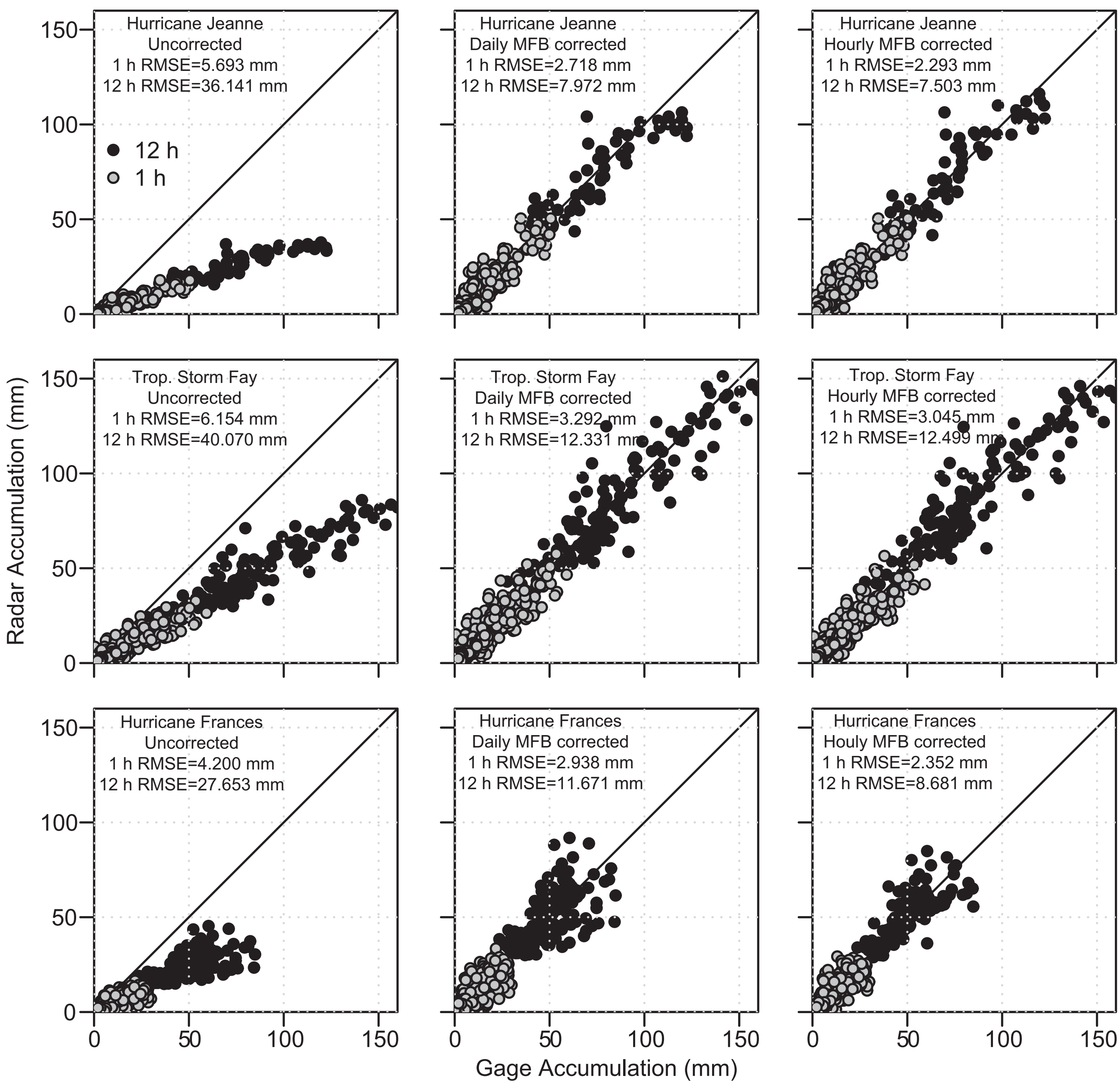

FIGURE 9. Scatterplots of Charlotte Raingage Network Rain Gage Accumulations to Corresponding Hydro-NEXRAD Radar Rainfall Accumulations for Three Tropical Storms. Top panels: Hurricane Jeanne, 27-28 September 2004. Middle panels: Tropical Storm Fay, 26-27 August 2008. Bottom panels: Hurricane Frances, 7-8 September 2004. Radar datasets shown are uncorrected Hydro-NEXRAD (left panels), Hydro-NEXRAD with daily mean field bias (MFB) correction (center panels), and Hydro-NEXRAD with hourly MFB correction (right panels). Grey filled circles are 1-h accumulations, black circles are 12-h accumulations. RMSE, root-mean-square error.

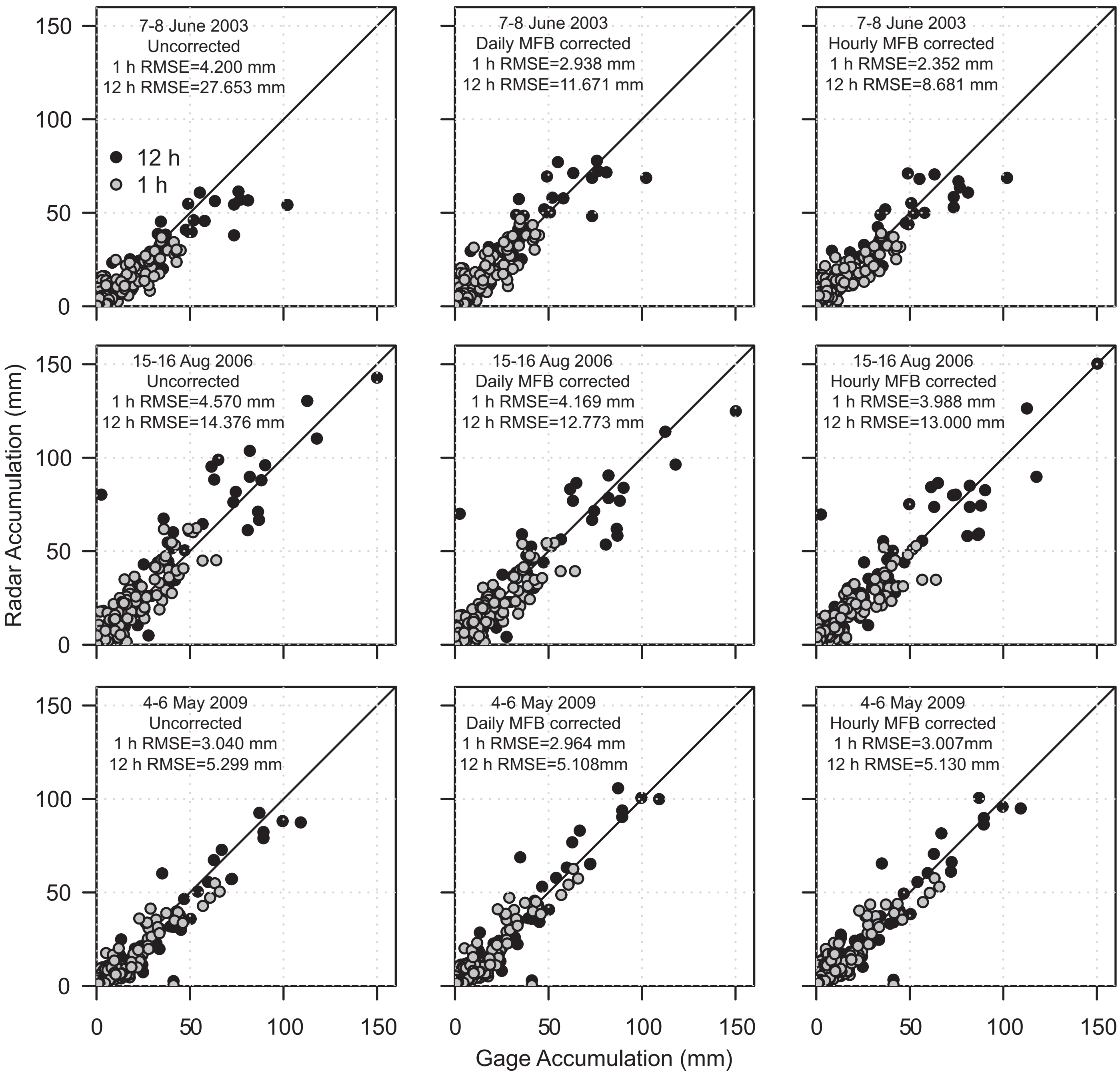

FIGURE 10. Scatterplots of Charlotte Raingage Network Rain Gage Accumulations to Corresponding Hydro-NEXRAD Radar Rainfall Accumulations for Three Nontropical Storms. Top panels: 7-8 June 2003. Middle panels: 15-16 August 2006. Bottom panels: 4-6 May 2009. Radar datasets shown are uncorrected Hydro-NEXRAD (left panels), Hydro-NEXRAD with daily mean field bias (MFB) correction (center panels), and Hydro-NEXRAD with hourly MFB correction (right panels). Grey filled circles are 1-h accumulations, black circles are 12-h accumulations. RMSE, root-mean-square error.

for the Hydro-NEXRAD reflectivity-to-rain rate conversion would likely yield better uncorrected estimates for rainfall associated with the tropical cyclones (see Villarini *et al.*, 2010 for results using the tropical *Z-R* for Hurricane Frances). MFB correction, however, effectively eliminates this underestimation (Figure 9, center and right panels), obviating the need for storm type-dependent *Z-R* relationships. There is some improvement for both 1- and 12-h accumulation periods for the Hydro-NEXRAD estimates that have been bias-corrected at the hourly scale rather than at the daily scale, particularly for Hurricane Frances. Accumulations for Hurricane Frances have more scatter than for the other two

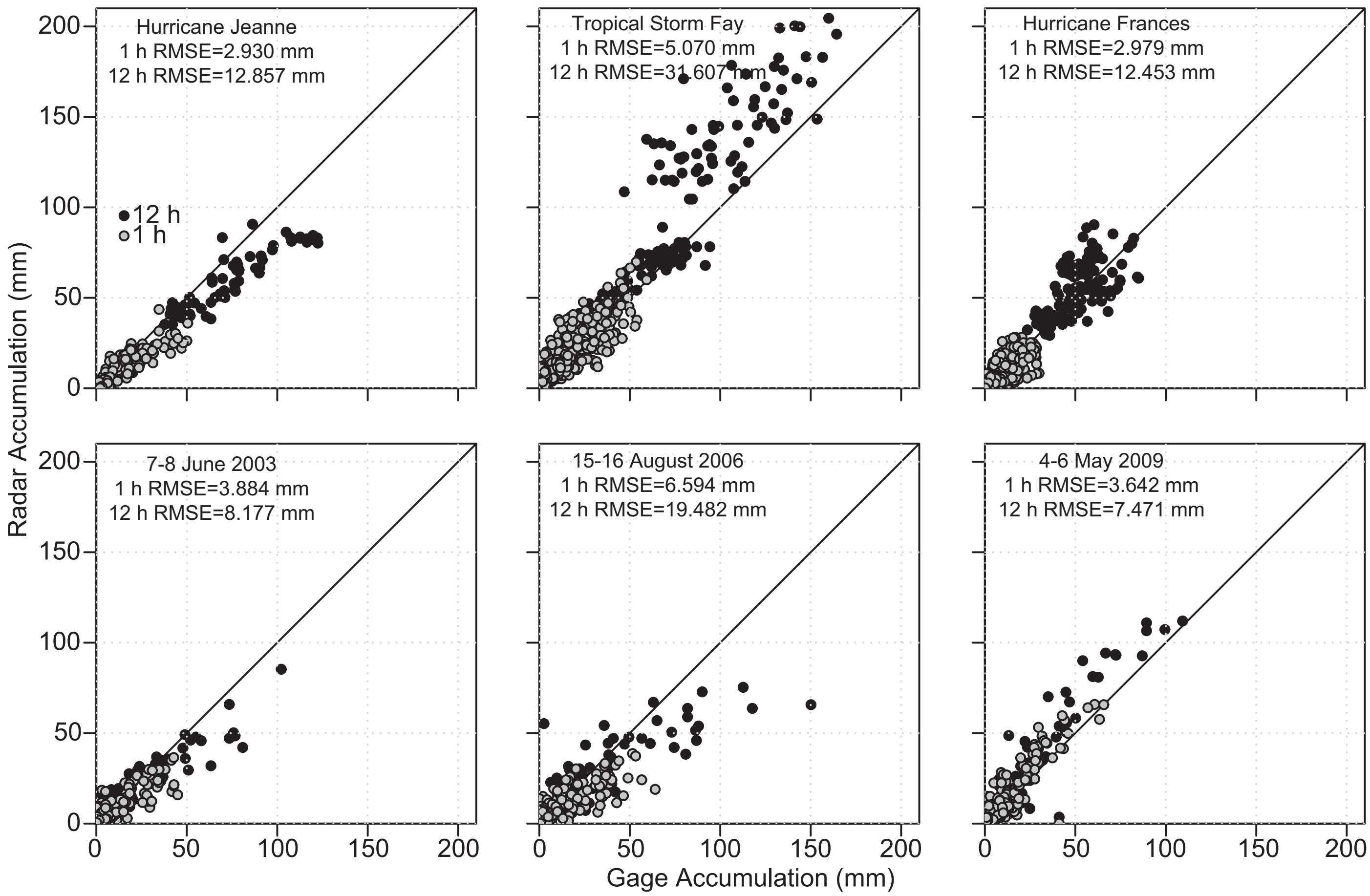

FIGURE 11. Scatterplots of Charlotte Raingage Network Rain Gage Accumulations to Corresponding Stage IV Multisensor Rainfall Accumulations for Three Tropical and Three Nontropical Storms. Top left: Hurricane Jeanne, 27-28 September 2004. Top center: Tropical Storm Fay, 26-27 August 2008. Top right: Hurricane Frances, 7-8 September 2004. Bottom left: 7-8 June 2003. Bottom center: 15-16 August 2006. Bottom right: 4-6 May 2009. Grey filled circles are 1-h accumulations, black circles are 12-h accumulations. RMSE, root-mean-square error.

tropical cyclones at both the 1- and the 12-h time scale. Hourly MFB correction yields lower RMSE than daily MFB correction for 1-h accumulations for all three storms, while 12-h RMSE is comparable and in fact is lower with daily MFB correction for Tropical Storm Jeanne.

Scatterplots of uncorrected 1- and 12-h Hydro-NEXRAD radar rainfall versus rain gage accumulations for the nontropical storms (Figure 10, left panels) contrast with those of the tropical systems. Uncorrected radar rainfall accumulations show much less bias for nontropical rainfall than for tropical cyclone rainfall, especially at the 12-h scale (Figure 10, center and right panels) and differences between the uncorrected and bias-corrected radar datasets are significantly less. There is little difference between the rainfall accumulations for the radar rainfall fields corrected at the daily versus hourly scales. The 1- and 12-h RMSE are lower for daily, rather than hourly, MFB correction for the 4-6 May 2009 event, as well as 12-h RMSE for 15-16 August 2006. For the remainder of the time periods, hourly MFB correction produces somewhat lower RMSE. The results of these six events suggest that despite the fact that tropical storms are often characterized by relatively long storm durations and large spatial extents, subdaily variability in atmospheric and rainfall properties that affect radar estimation are more pronounced than in nontropical storms (see also Smith *et al.*, 2005b).

Scatterplots of 1- and 12-h Stage IV rainfall accumulations show large variability in bias compared to the corrected Hydro-NEXRAD datasets (Figure 11). Stage IV tends to underestimate rainfall for Hurricane Jeanne and for the June 2003 and August 2006 storms, and to overestimate for Tropical Storm Fay and for the May 2009 storm. Because the *Z-R* selection and multi-sensor merging is performed in near-realtime at the RFC and can be influenced by the subjectivity of the operator and the quality of incoming gage observations, it is very difficult to assess the underlying causes for biases in Stage IV rainfall estimates. Some of the bias evident in the Stage IV data may be attributable to its coarser resolution since it may not capture the sharp spatial rainfall gradients in convective cells that produce high rain rates in nontropical storms as effectively as the higher-resolution Hydro-NEXRAD. Stage IV 12-h RMSE is actually lower than either bias-corrected Hydro-NEXRAD dataset for 7-6 June 2003, but is higher for every other event.

Time series plots of basin-averaged rainfall and discharge observations illustrate the variability of rainfall and discharge and the importance of timing for urban flooding (Figures 12 and 13). Bias-corrected Hydro-NEXRAD datasets underestimate high basin-averaged rain rates for Little Hope Creek (6.7 km^2) relative to the CRN IDW-interpolated estimates for Hurricane Jeanne (Figure 12, top panel; Stage IV time series omitted for clarity) and vice versa for Little Sugar Creek at Archdale (Figure 12, bottom panel; Stage IV time series omitted for clarity). Examination of rainfall time series for other events does not reveal systematic structure to the relative magnitudes of gage-interpolated and Hydro-NEXRAD basin-averaged rainfall rates as a function of event type, basin size, or any other factor (results not shown). The lack of evident systematic differences in the rain gage and Hydro-NEXRAD basin-averaged time series suggests that CB at the basin scale is minimal. In all cases, the temporal structure of radar rainfall estimates is roughly consistent with the interpolated CRN, especially for Little Sugar Creek at Archdale (110 km^2). The precise timing of the gage-estimated rainfall may be erroneous in Little Hope Creek since there are no gages in the central part of the basin, and so storm movement over the basin may not be properly represented.

Basin-averaged rainfall time series and discharge for the June 8, 2003 storm (nontropical) illustrate the importance of high temporal resolution for urban flooding (Figure 13, CRN time series is omitted for clarity). The elapsed time between peak rainfall and peak discharge for Little Sugar Creek at Medical Center is shorter than for Little Hope Creek, consistent with the analyses presented in Table 5. In addition, the peak discharge for Little Sugar Creek at Medical Center, which occurs at about 02:15 UTC, occurs in response to a second small rainfall pulse lasting from 1:30 to 2:00 UTC. A hydrologic model forced with coarse temporal resolution Stage IV data would not be capable of capturing this rise in discharge due to the second rainfall pulse, and thus would not be capable of simulating the peak discharge for the event.

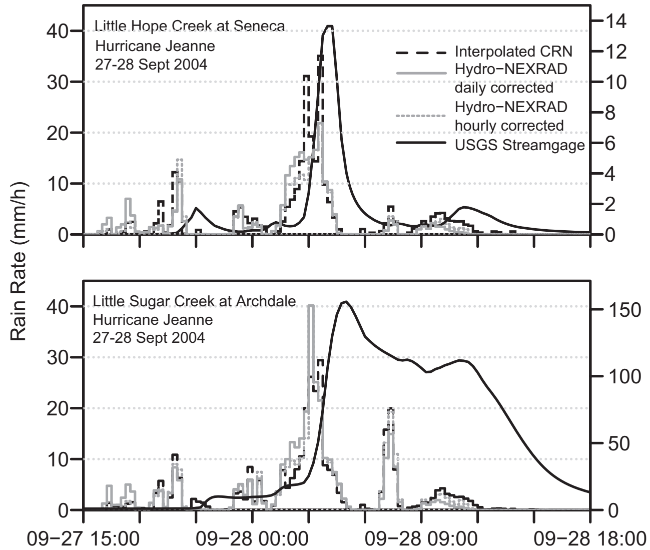

FIGURE 12. Basin-Average Rainfall for Hydro-NEXRAD with Mean Field Bias Correction Done at the Daily and Hourly Scales, Interpolated Charlotte Raingage Network (CRN) Rain Gages, and USGS Discharge Time Series for Hurricane Jeanne, 27-28 September 2004 for Little Hope Creek (top panel) and Little Sugar Creek at Archdale (bottom panel). All times are in Coordinated Universal Time.

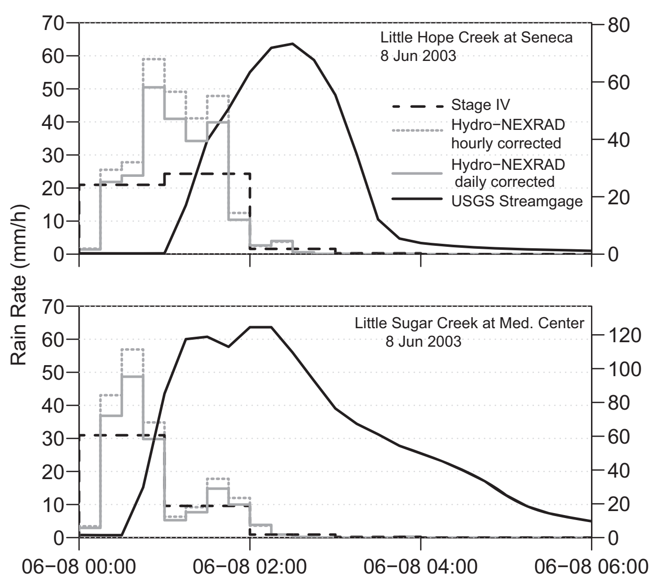

FIGURE 13. Basin-Average Rainfall for Hydro-NEXRAD with Mean Field Bias Correction Done at the Daily and Hourly Scales, Stage IV, and U.S. Geological Survey (USGS) Discharge for 7 June 2003 Nontropical Storm for Little Hope Creek (top panel) and Little Sugar Creek at Medical Center (bottom panel). All times are in Coordinated Universal Time.

SUMMARY AND CONCLUSIONS

This study examines long-term (10-year) high-resolution (1 km^2, 15-min) bias-corrected radar rainfall datasets developed using the Hydro-NEXRAD processing system, focusing on their applications to urban hydrology. The main findings of this study are:

1. Systematic errors in calibration and *Z-R* relationships can lead to multiplicative biases in radar rainfall estimates. MFB correction using a rain gage network can substantially reduce these biases. MFB correction performed at the daily scale is often, but not always, comparable in accuracy to MFB correction performed at the hourly scale. Thus, the fact that many rain gage data are available only at the daily scale is not a major limitation to their usefulness for bias correction of radar rainfall fields. Rainfall estimation during the cold season is more challenging than during the warm season due to bright band enhancement of reflectivity and difficulties discriminating between frozen and liquid precipitation.
2. High-resolution (15-min, 1 km^2) bias-corrected rainfall estimates using the Hydro-NEXRAD processing system show better agreement with rain gage estimates than the NCEP Stage IV MPE product (hourly, 16 km^2). The higher spatial and temporal resolution of the Hydro-NEXRAD estimates is especially important in urban areas, where the relevant hydrologic processes are characterized by short time and length scales.
3. Conditional (rain rate-dependent) bias is still evident in Hydro-NEXRAD radar rainfall estimates after MFB correction. The KGSP radar tends to underestimate high rainfall rates relative to rain gage observations. The magnitude of CB decreases with increasing accumulation period. CB can be explicitly eliminated but only at the expense of other performance criteria such as RMSE and MAE. The use of CB correction may therefore depend on the application, and more investigation is necessary to determine for which applications CB correction may or may not be appropriate.
4. The spatial and temporal structure of Hydro-NEXRAD radar rainfall fields is similar to that of rain gage-estimated rainfall, and observable differences are likely attributable to the sampling properties of the two instruments. Both spatial and temporal correlation for radar and gage-estimated rainfall is lower in the warm season than in the cold season, since warm-season precipitation in the Southeastern U.S. is characterized by sharp spatial rainfall gradients associated with convective storms. The temporal correlation of MFB, however, is lower during the cold season than during the warm season, suggesting that the measurement of cold-season precipitation using radar is a major challenge and that subdaily bias correction may be more important in the cold season than in the warm season.
5. Approximately 25 rain gages over a 2,500 km^2 area are adequate to accurately estimate MFB at the daily scale in the Charlotte area. Many urban areas in the U.S. and elsewhere have similar gage densities, suggesting that MFB correction of radar rainfall for many urban areas is feasible, even in locations where there are insufficient numbers of gages to accurately obtain direct high-resolution gage-based measurements of rainfall over large areas. More work is needed to determine how these results can be generalized to other settings and to different time scales.
6. Response times, computed from rainfall and runoff for 50 flood events for three basins ranging in size from 6.7 to 110 km^2, vary depending on the rainfall dataset used. Response times based on the Stage IV radar rainfall product are longer than for the higher-resolution rainfall datasets, suggesting that Stage IV rainfall data may not be adequate for applications such as flood hydrologic modeling in which precise timing is critical. Response times calculated from the Hydro-NEXRAD datasets are comparable to those calculated from a dense gage network.
7. Storm event water balance computations for 50 storms using basin-averaged rainfall estimates and corresponding USGS discharge for the three study basins vary by rainfall dataset. Hydro-NEXRAD fields with daily MFB correction yield similar rainfall depths to fields with hourly MFB correction. Rainfall depths from bias corrected Hydro-NEXRAD fields are comparable to those calculated from the dense rain gage network except at short time periods (1-h) for Little Hope Creek, the smallest basin. This discrepancy may be due to CB in radar estimates, which is more prevalent at short time scales, or to poor rain gage coverage in Little Hope Creek. For accumulation periods greater than 1 h, Stage IV rainfall estimates and runoff ratios, as well as corresponding variability, are broadly consistent with other datasets. The variability of the rain gage-interpolated rainfall depths is lower than for the other datasets for most watersheds and most time periods, possibly due to the effects of the smoothing resulting from the interpolation routine. More sophisticated interpolation schemes may yield more realistic variability, but would require additional assumptions regarding rainfall structure. Due to the continuous spatial sampling, radar rainfall fields do not require such assumptions.

8. In-depth examination of three tropical and three nontropical storm systems reveal that uncorrected Hydro-NEXRAD using the standard *Z-R* relationship severely underestimates extreme rainfall from tropical storms. This underestimation is much less pronounced for nontropical storms. MFB correction at either the daily or hourly scale effectively eliminates systematic bias for both tropical and nontropical storms, suggesting that if MFB is used, it is not necessary to vary the *Z-R* relationship according to storm type. Hourly MFB correction provides slight improvements over daily MFB correction in rainfall estimates for tropical storms, while the two bias correction timescales are equivalent for nontropical storms. This suggests that the variability in atmospheric and rainfall properties of tropical storms that affect radar rainfall estimation is more prominent than in nontropical storms. Bias in Stage IV estimates ranges from substantial underestimation to substantial overestimation with no apparent relation to storm type.
9. Examination of time series of basin-average rainfall and of streamflow show that there is no systematic temporal structure to differences in basin-averaged rainfall estimates from rain gages and bias-corrected Hydro-NEXRAD radar rainfall fields, and that both rain rate magnitude and timing generally agree between the gages and the bias-corrected radar rainfall. The coarser-resolution Stage IV does not capture the temporal structure of flood producing rainfall. Dual-polarization upgrades to the NEXRAD network were completed in 2012 and are an important step forward in precipitation estimation using radar, with the potential to reduce or eliminate the need for bias correction and especially to improve cold season precipitation estimation. It will be a long time, however, before polarimetric radar records approach the length of existing single-polarization NEXRAD data records, so existing single-polarization archives combined with bias correction will continue to be a valuable resource for hydrologists well into the next decade.

In conclusion, we have demonstrated that bias-corrected high-resolution radar rainfall fields such as those from Hydro-NEXRAD can be comparable to or better than observations from dense rain gage networks, and have major advantages over coarser resolution multi-sensor products such as NCEP Stage IV. This is particularly important in areas that lack dense gage coverage. The spatially continuous sampling of rainfall over large areas means that radar can provide information that is useful both for researchers and practitioners. Questions remain such as how to deal with CB and how to improve the measurement of cold season precipitation, but high-resolution radar rainfall can and should play a larger role in urban hydrology. The long-term bias corrected datasets will be made available to other researchers by request, and we encourage practitioners to examine the possible role of radar rainfall in their work.

ACKNOWLEDGMENTS

This work was partially funded by the Willis Research Network, the NOAA Cooperative Institute for Climate Sciences (Grant NOAA CICS NA08OAR4320752), and the National Science Foundation (Grant CBET-1058027). We would like to thank Wendi Young from the USGS Charlotte office for providing CRN data and Dena Feldman from Princeton University for her thoughtful revisions. Finally, we acknowledge the criticisms and suggestions of the three anonymous reviewers.

LITERATURE CITED

Anagnostou, E.N., W.F. Krajewski, and J.A. Smith, 1999. Uncertainty Quantification of Mean-Areal Radar-Rainfall Estimates. The Journal of Atmospheric and Oceanic Technology 16:206-215.

Andrieu, H. and J.D. Creutin, 1995. Identification of Vertical Profiles of Radar Reflectivity for Hydrological Applications Using an Inverse Method. Part I: Formulation. Journal of Applied Meteorology 34:225-239.

Baeck, M.L. and J.A. Smith, 1998. Rainfall Estimation by the WSR-88D for Heavy Rainfall Events. Weather and Forecasting 13:416-436.

Bedient, P., B. Hoblit, D. Gladwell, and B. Vieux, 2000. NEXRAD Radar for Flood Prediction in Houston. Journal of Hydrologic Engineering 5:269-277.

Bellon, A., G. Lee, A. Kilambi, and I. Zawadski, 2007. Real-Time Comparisons of VPR-Corrected Daily Rainfall Estimates with a Gauge Mesonet. Journal of Applied Meteorology and Climatology 46:726-741.

Berne, A., G. Delrieu, H. Andrieu, and J. Creutin, 2004a. Influence of the Vertical Profile of Reflectivity on Radar-Estimated Rain Rates at Short Time Steps. Journal of Hydrometeorology 5:296-310.

Berne, A., G. Delrieu, J.-D. Creutin, and C. Obled, 2004b. Temporal and Spatial Resolution of Rainfall Measurements Required for Urban Hydrology. Journal of Hydrology 299(3-4):166-179.

Borga, M., 2002. Accuracy of Radar Rainfall Estimates for Streamflow Simulation. Journal of Hydrology 267:26-39.

Borga, M., S. Degli Esposti, and D. Norbiato, 2006. Influence of Errors in Radar Rainfall Estimates on Hydrological Modeling Prediction Uncertainty. Water Resources Research 42:W08409.

Borga, M., F. Tonelli, R.J. Moore, and H. Andrieu, 2002. Long-Term Assessment of Bias Adjustment in Radar Rainfall Estimation. Water Resources Research 38:1226.

Bornstein, R. and Q. Lin, 2000. Urban Heat Islands and Summertime Convective Thunderstorms in Atlanta: Three Case Studies. Atmospheric Environment 34:507-516.

Changnon, S., 1979. Rainfall Changes in Summer Caused by St Louis. Science 205:402-404.

Changnon, S.A.J., F.A. Huff, and R.G. Semonin, 1971. METROMEX: An Investigation of Inadvertent Weather Modification. Bulletin of the American Meteorological Society 52:958-968.

Ciach, G.J., 2003. Local Random Errors in Tipping-Bucket Rain Gauge Measurements. Journal of Atmospheric and Oceanic Technology 20:752-759.

Ciach, G.J. and W.F. Krajewski, 1999. On the Estimation of Radar Rainfall Error Variance. Advances in Water Resources 22:585-595.

Ciach, G.J., W.F. Krajewski, and G. Villarini, 2007. Product-Error-Driven Uncertainty Model for Probabilistic Quantitative Precipitation Estimation with NEXRAD Data. Journal of Hydrometeorology 8:1325-1347.

Ciach, G.J., M.L. Morrissey, and W.F. Krajewski, 2000. Conditional Bias in Radar Rainfall Estimation. Journal of Applied Meteorology 39:1941-1946.

Cleveland, W., 1979. Robust Locally Weighted Regression and Smoothing Scatterplots. Journal of the American Statistical Association 74:829-836.

Creutin, J.D., M. Borga, C. Lutoff, A. Scolobig, I. Ruin, and L. Créton-Cazanave, 2009. Catchment Dynamics and Social Response During Flash Floods: The Potential of Radar Rainfall Monitoring for Warning Procedures. Meteorological Applications 16:115-125.

Cunha, L.K., P.V. Mandapaka, W.F. Krajewski, R. Mantilla, and A.A. Bradley, 2012. Impact of Radar-Rainfall Error Structure on Estimated Flood Magnitude Across Scales: An Investigation Based on a Parsimonious Distributed Hydrological Model. Water Resources Research 48(10):W10515.

Diem, J.E., 2008. Detecting Summer Rainfall Enhancement within Metropolitan Atlanta, Georgia USA. International Journal of Climatology 28:129-133.

Diem, J.E. and T.L. Mote, 2005. Interepochal Changes in Summer Precipitation in the Southeastern United States: Evidence of Possible Urban Effects near Atlanta, Georgia. Journal of Applied Meteorology 44:717-730.

Einfalt, T., K. Arnbjerg-Nielsen, C. Golz, N.-E. Jensen, M. Quirmbach, G. Vaes, and B. Vieux, 2004. Towards a Roadmap for Use of Radar Rainfall Data in Urban Drainage. Journal of Hydrology 299:186-202.

El Hassan, A.A., H.O. Sharif, T. Jackson, and S. Chintalapudi, 2012. Performance of a Conceptual and Physically Based Model in Simulating the Response of a Semiurbanized Watershed in San Antonio, Texas. Hydrological Processes, doi: 10.1002/hyp.9443.

Emmanuel, I., H. Andrieu, and P. Tabary, 2012. Evaluation of the New French Operational Weather Radar Product for the Field of Urban Hydrology. Atmospheric Research 103:20-32.

Fulton, R.A., J.P. Breidenbach, D.-J. Seo, D.A. Miller, and T. O'Bannon, 1998. The WSR-88D Rainfall Algorithm. Weather and Forecasting 13:377-395.

Germann, U., M. Berenguer, D. Sempere-Torres, and M. Zappa, 2009. REAL—Ensemble Radar Precipitation Estimation for Hydrology in a Mountainous Region. Quarterly Journal of the Royal Meteorological Society 135:445-456.

Germann, U., G. Galli, M. Boscacci, and M. Bolliger, 2006. Radar Precipitation Measurement in a Mountainous Region. Quarterly Journal of the Royal Meteorological Society 132:1669-1692.

Gourley, J.J. and B.E. Vieux, 2005. A Method for Evaluating the Accuracy of Quantitative Precipitation Estimates from a Hydrologic Modeling Perspective. Journal of Hydrometeorology 6:115-133.

Habib, E., A.V. Aduvala, and E.A. Meselhe, 2008. Analysis of Radar-Rainfall Error Characteristics and Implications for Streamflow Simulation Uncertainty. Hydrological Sciences Journal 53:568-587.

Habib, E., W. Krajewski, and A. Kruger, 2001. Sampling Errors of Tipping-Bucket Rain Gauge Measurements. Journal of Hydrologic Engineering 6:159-166.

Habib, E., B.F. Larson, and J. Graschel, 2009. Validation of NEXRAD Multisensory Precipitation Estimates Using an Experimental Dense Rain Gauge Network in South Louisiana. Journal of Hydrology 373:463-478.

Hart, R.E. and J.L. Evans, 2001. A Climatology of the Extratropical Transition of Atlantic Tropical Cyclones. Journal of Climate 14:546-564.

Hazenberg, P., N. Yu, B. Boudevillain, G. Delrieu, and R. Uijlenhoet, 2011. Scaling of Raindrop Size Distributions and Classification of Radar Reflectivity-Rain Rate Relations in Intense Mediterranean Precipitation. Journal of Hydrology 402:179-192.

Heiss, W.H., D.L. McGrew, and D. Sirmans, 1990. NEXRAD-Next Generation Weather Radar (WSR-88D). Microwave Journal 33:79.

Hjelmfelt, M.R., 1982. Numerical Simulation of the Effects of St. Louis on Mesoscale Boundary-Layer Airflow and Vertical Air Motion: Simulations of Urban vs. Non-Urban Effects. Journal of Applied Meteorology 21:1239-1257.

Hossain, F., E.N. Anagnostou, T. Dinku, and M. Borga, 2004. Hydrological Model Sensitivity to Parameter and Radar Rainfall Estimation Uncertainty. Hydrological Processes 18:3277-3291.

Huff, F.A. and J.L. Vogel, 1978. Urban, Topographic and Diurnal Effects on Rainfall in the St. Louis Region. Journal of Applied Meteorology 17:565-577.

Jarvinen, B.R., C.J. Neumann, and M.A.S. Davis, 1984. A Tropical Cyclone Data Tape for the North Atlantic Basin, 1886-1983: Contents, Limitations, and Uses. Technical Report, National Oceanic and Atmospheric Administration, National Hurricane Center, Miami, Florida, 24 pp.

Kirstetter, P.-E., G. Delrieu, B. Boudevillain, and C. Obled, 2010. Toward an Error Model for Radar Quantitative Precipitation Estimation in the Cévennes-Vivarais Region, France. Journal of Hydrology 394:28-41.

Krajewski, W. and J.A. Smith, 2002. Radar Hydrology: Rainfall Estimation. Advances in Water Resources 25:1387-1394.

Krajewski, W., G. Villarini, and J.A. Smith, 2010a. Radar-Rainfall Uncertainties: Where Are We after Thirty Years of Effort? Bulletin of the American Meteorological Society 91:87-94.

Krajewski, W.F., A. Kruger, J.A. Smith, R. Lawrence, C. Gunyon, R. Goska, B.C. Seo, P. Domaszczynski, M.L. Baeck, M.K. Ramamurthy, J. Weber, A.A. Bradley, S.A. DelGreco, and M. Steiner, 2010b. Towards Better Utilization of NEXRAD Data in Hydrology: An Overview of Hydro-NEXRAD. Journal of Hydroinformatics 13(2):255-266.

Krajewski, W.F., B. Vignal, B.C. Seo, and G. Villarini, 2011. Statistical Model of the Range-Dependent Error in Radar-Rainfall Estimates Due to the Vertical Profile of Reflectivity. Journal of Hydrology 402:306-316.

Kunkel, K.E., D.R. Easterling, D.A.R. Kristovich, B. Gleason, L. Stoecker, and R. Smith, 2011. Recent Increases in U.S. Heavy Precipitation Associated with Tropical Cyclones. Geophysical Research Letters 37:L24706.

Looper, J.P. and B.E. Vieux, 2012. An Assessment of Distributed Flash Flood Forecasting Accuracy Using Radar and Rain Gauge Input for a Physics-Based Distributed Hydrologic Model. Journal of Hydrology 412-413:114-132.

Meierdiercks, K.L., J.A. Smith, M.L. Baeck, and A.J. Miller, 2010. Analyses of Urban Drainage Network Structure and Its Impact on Hydrologic Response. Journal of the American Water Resources Association 46:932-943.

Moore, R.J., D.A. Jones, D.R. Cox, and V.S. Isham, 2000. Design of HYREX Rain Gage Network. Hydrology and Earth Systems Sciences 4:521-530.

Mote, T.L., M.C. Lacke, and J.M. Shepherd, 2007. Radar Signatures of the Urban Effect on Precipitation Distribution: A Case Study for Atlanta, Georgia. Geophysical Research Letters 34:L20710.

Murphy, M.S. and C.E. Konrad, 2005. Spatial and Temporal Patterns of Thunderstorm Events That Produce Cloud-to-Ground Lightning in the Interior Southeastern United States. Monthly Weather Review 133:1417-1430.

Neumann, C.J., B.R. Jarvinen, C.J. McAdie, and J.D. Elms, 1993. Tropical Cyclones of the North Atlantic Ocean. Technical Report, National Climatic Data Center/National Hurricane Center, Asheville, North Carolina, 193 pp.

Ntelekos, A.A., J.A. Smith, and W.F. Krajewski, 2007. Climatological Analyses of Thunderstorms and Flash Floods in the Baltimore Metropolitan Region. Journal of Hydrometeorology 8:88-101.

Overeem, A., I. Holleman, and A. Buishand, 2009. Derivation of a 10-Year Radar-Based Climatology of Rainfall. Journal of Applied Meteorology and Climatology 48:1448-1463.

Rinehart, R.E., 2004. Radar for Meteorologists (Fourth Edition). Rinehart Publications, Columbia, Missouri, ISBN-13: 978-0965800211.

Rodriguez-Iturbe, I. and J.M. Mejia, 1974. The Design of Rainfall Networks in Time and Space. Water Resources Research 10:713-728.

Rose, L.S., J.A. Stallins, and M.L. Bentley, 2008. Concurrent Cloud-to-Ground Lightning and Precipitation Enhancement in the Atlanta, Georgia (United States), Urban Region. Earth Interactions 12:1-30.

Schilling, W., 1991. Rainfall Data for Urban Hydrology: What Do We Need? Atmospheric Research 27(1-3):5-21.

Schröter, K., X. Llort, C. Velasco-Forero, M. Ostrowski, and D. Sempere-Torres, 2011. Implications of Radar Rainfall Estimates Uncertainty on Distributed Hydrological Model Predictions. Atmospheric Research 100:237-245.

Seo, D., J. Breidenbach, R. Fulton, and D. Miller, 2000. Real-Time Adjustment of Range-Dependent Biases in WSR-88D Rainfall Estimates Due to Nonuniform Vertical Profile of Reflectivity. Journal of Hydrometeorology 1:222-240.

Seo, D.J., 1998. Real-Time Estimation of Rainfall Fields Using Radar Rainfall and Rain Gage Data. Journal of Hydrology 208:37-52.

Seo, D.J., J.P. Breidenbach, and E.R. Johnson, 1999. Real-Time Estimation of Mean Field Bias in Radar Rainfall Data. Journal of Hydrology 223:131-147.

Sharif, H., L. Sparks, A. Hassan, J. Zeitler, and H. Xie, 2010a. Application of a Distributed Hydrologic Model to the November 17, 2004, Flood of Bull Creek Watershed, Austin, Texas. Journal of Hydrologic Engineering 15:651-657.

Sharif, H.O., A.A. Hassan, S. Bin-Shafique, H. Xie, and J. Zeitler, 2010b. Hydrologic Modeling of an Extreme Flood in the Guadalupe River in Texas. Journal of the American Water Resources Association 46:881-891.

Shepherd, M.J., H. Pierce, and A.J. Negri, 2002. Rainfall Modification by Major Urban Areas: Observations from Spaceborne Rain Radar on the TRMM Satellite. Journal of Applied Meteorology 41:689-701.

Smith, B.K., J.A. Smith, M.L. Baeck, G. Villarini, and D.B. Wright, 2013. The Spectrum of Storm Event Hydrologic Response in Urban Watersheds. Water Resources Research 29:2649-2663.

Smith, J.A., M.L. Baeck, K.L. Meierdiercks, A.J. Miller, and W.F. Krajewski, 2007. Radar Rainfall Estimation for Flash Flood Forecasting in Small Urban Watersheds. Advances in Water Resources 30:2087-2097.

Smith, J.A., M.L. Baeck, J.E. Morrison, P. Sturdevant-Rees, D.F. Turner-Gillespie, and P.D. Bates, 2002. The Regional Hydrology of Extreme Floods in an Urbanizing Drainage Basin. Journal of Hydrometeorology 3:267-282.

Smith, J.A., M.L. Baeck, G. Villarini, C. Welty, A.J. Miller, and W.F. Krajewski, 2012. Analyses of a Long-Term High-Resolution Radar Rainfall Data Set for the Baltimore Metropolitan Region. Water Resources Research 48:W04504.

Smith, J.A. and W.F. Krajewski, 1991. Estimation of the Mean Field Bias of Radar Rainfall Estimates. Journal of Applied Meteorology 30:397-412.

Smith, J.A., A.J. Miller, M.L. Baeck, P.A. Nelson, G.T. Fisher, and K.L. Meierdiercks, 2005a. Extraordinary Flood Response of a Small Urban Watershed to Short Duration Convective Rainfall. Journal of Hydrometeorology 6:599-617.

Smith, J.A., P. Sturdevant-Rees, M.L. Baeck, and M.C. Larsen, 2005b. Tropical Cyclones and the Flood Hydrology of Puerto Rico. Water Resources Research 41(6):W06020.

Steiner, M. and J.A. Smith, 2002. Use of Three-Dimensional Reflectivity Structure for Automated Detection and Removal of Nonprecipitating Echoes in Radar Data. Journal of Atmospheric and Oceanic Technology 19:673-686.

Thielen, J., W. Wobrock, A. Gadian, P. Mestayer, and J.-D. Creutin, 2000. The Possible Influence of Urban Surfaces on Rainfall Development: A Sensitivity Study in 2D in the Meso-Gamma-Scale. Atmospheric Research 54:15-39.

Thol, P.T., 1972. The Relative Efficiency of the Density of Rain-Gage Networks. Journal of Hydrology 15:193-208.

Turner-Gillespie, D.F., J.A. Smith, and P.D. Bates, 2003. Attenuating Reaches and the Regional Flood Response of an Urbanizing Drainage Basin. Advances in Water Resources 26:673-684.

Vieux, B.E. and P.B. Bedient, 2004. Assessing Urban Hydrologic Prediction Accuracy through Event Reconstruction. Journal of Hydrology 299:217-236.

Vieux, B.E. and J. Imgarten, 2012. On the Scale-Dependent Propagation of Hydrologic Uncertainty Using High-Resolution X-Band Radar Rainfall Estimates. Atmospheric Research 103:96-105.

Vieux, B.E. and J.E. Vieux, 2005. Statistical Evaluation of a Radar Rainfall System for Sewer System Management. Atmospheric Research 77:322-336.

Vignal, B. and W.F. Krajewski, 2001. Large-Sample Evaluation of Two Methods to Correct Range-Dependent Error for WSR-88D Rainfall Estimates. Journal of Hydrometeorology 2:490-504.

Villarini, G. and W.F. Krajewski, 2009. Empirically Based Modeling of Radar-Rainfall Uncertainties for a C-Band Radar at Different Time-Scales. Quarterly Journal of the Royal Meteorological Society 135:1424-1438.

Villarini, G. and W.F. Krajewski, 2010a. Sensitivity Studies of the Models of Radar-Rainfall Uncertainties. Journal of Applied Meteorology and Climatology 49:288-309.

Villarini, G. and W.F. Krajewski, 2010b. Review of the Different Sources of Uncertainty in Single Polarization Radar-Based Estimates of Rainfall. Surveys in Geophysics 31:107-129.

Villarini, G., P.V. Mandapaka, W.F. Krajewski, and R.J. Moore, 2008a. Rainfall and Sampling Uncertainties: A Rain Gauge Perspective. Journal of Geophysical Research 113:D11102.

Villarini, G., F. Serinaldi, and W.F. Krajewski, 2008b. Modeling Radar-Rainfall Estimation Uncertainties Using Parametric and Non-Parametric Approaches. Advances in Water Resources 31:1674-1686.

Villarini, G. and J.A. Smith, 2010. Flood Peak Distributions for the Eastern United States. Water Resources Research 46:W06504.

Villarini, G., J.A. Smith, M.L. Baeck, T. Marchock, and G.A. Vecchi, 2011. Characterization of Rainfall Distribution and Flooding Associated with U.S. Landfalling Tropical Cyclones: Analyses of Hurricanes Frances, Ivan, and Jeanne (2004). Journal of Geophysical Research 116:D23116.

Villarini, G., J.A. Smith, M.L. Baeck, B.K. Smith, and P. Sturdevant-Rees, 2013. Hydrologic Analyses of the 17-18 July 1996 Flood in Chicago and the Role of Urbanization. Journal of Hydrologic Engineering 18(2):250-259.

Villarini, G., J.A. Smith, M.L. Baeck, P. Sturdevant-Rees, and W.F. Krajewski, 2010. Radar Analyses of Extreme Rainfall and Flooding in Urban Drainage Basins. Journal of Hydrology 381:266-286.

Weisman, R.A., 1990a. An Observational Study of Warm Season Southern Appalachian Lee Troughs. Part I: Boundary Layer Circulation. Monthly Weather Review 118:950.

Weisman, R.A., 1990b. An Observational Study of Warm Season Southern Appalachian Lee Troughs. Part II: Thunderstorm Genesis Zones. Monthly Weather Review 118:2020.

Westcott, N.E., H.V. Knapp, and S.D. Hilberg, 2008. Comparison of Gage and Multi-Sensor Precipitation Estimates over a Range of Spatial and Temporal Scales in the Midwestern United States. Journal of Hydrology 351:1-12.

Wilson, J.W. and E.A. Brandes, 1979. Radar Measurement of Rainfall—A Summary. Bulletin of the American Meteorological Society 60:1048-1058.

Wright, D.B., J.A. Smith, G. Villarini, and M.L. Baeck, 2012. The Hydroclimatology of Flash Flooding in Atlanta. Water Resources Research 48:W04524

Wright, D.B., J.A. Smith, G. Villarini, and M.L. Baeck, 2013. Estimating the Frequency of Extreme Rainfall Using Weather Radar and Stochastic Storm Transposition. Journal of Hydrology 488:150-165.

Yang, L., J.A. Smith, D.B. Wright, M.L. Baeck, G. Villarini, F. Tian, and H. Hu, 2013. Urbanization and Climate Change: An Examination of Nonstationarities in Flood Frequency. Journal of Hydrometeorology. http://journals.ametsoc.org/doi/abs/10.1175/JHM-D-12-095.1, *accessed* October 2013.